

typical spongiform change consisting of fine vacuole-type (microvacuolar pattern with multiple single-rounded spaces within the neuropil^{2,14}) and synaptic-type PrP deposition, characteristic of MM1-type sCJD,^{1,2} was not observed in the cerebral cortex. Because the present patient showed widespread cerebral neocortical involvement, we believe he exhibited a typical CJD clinical course. However, it was not apparent from the pathologic findings why this patient showed a rapidly progressive course, unlike other patients with MM2-cortical-type sCJD.

With respect to MM2-cortical-type sCJD, the mean age at onset is reported to be 65 years (range, 49–77 years) with an average disease duration of 16 months (range, 9–36 months).³ Myoclonus occurs as late as 8 months after symptom onset, often leading to the suspicion of sCJD.⁸ EEG characteristically shows non-specific slowing; occasional non-periodic paroxysmal discharges are observed.² Although PSWCs are not observed in most cases,^{2,3} a late occurrence of PSWCs was reported by Hamaguchi *et al.*¹⁰ Interestingly, the present patient showed only a 5-month disease duration but showed myoclonus and PSWCs on EEG. The clinical presentation of the present patient did not distinguish between MM2-cortical-type sCJD and typical sCJD.¹² The CSF NSE level was increased, but 14-3-3 protein was not examined. CSF 14-3-3 protein and NSE levels are reported to be increased in 70% of patients with MM2-cortical-type sCJD.^{8,11}

Hamaguchi *et al.*¹⁰ proposed the following diagnostic criteria for MM2-cortical-type sCJD on the basis of their observations and review of the literature: (i) progressive dementia; (ii) cortical hyperintensity on DWI; and (iii) increased CSF 14-3-3 protein level, with the exclusion of other dementias, including other types of prion disease. Neuropsychiatric abnormalities other than dementia or PSWCs are not necessarily required.¹⁰ Prolonged disease duration, a monosymptomatic disease course (mostly with isolated dementia) of at least 6 months and low sensitivity of EEG and MRI (with the exception of DWI) can result in delayed diagnosis of sCJD or in misdiagnosis as AD.⁸ Such misdiagnosis is clinically important because sufficient measures for preventing prion transmission are not taken with these patients. In the present case, cortical hyperintensity on DWI readily led to a diagnosis of possible CJD. Cortical hyperintensity on DWI is useful for the clinical diagnosis of sCJD.¹⁵ However, neurologic manifestations, such as the presence of myoclonus and PSWCs and an increase in CSF 14-3-3 protein, are often found in different sCJD subtypes¹⁵ and therefore cannot be considered specific for MM2-cortical-type sCJD.⁸ Krasnianski *et al.*⁸ reported that the sensitivity of cortical hyperintensity on DWI for MM2-cortical-type sCJD is not necessarily higher than that for other sCJD subtypes. However, other reports suggest that cortical hypersensitivity on DWI does have high diagnostic

sensitivity for the clinical diagnosis of MM2-cortical-type sCJD.^{9,10}

In the present case, the initial symptoms were memory disturbance and dementia. Aphasia, apraxia and pyramidal and extrapyramidal signs were also observed in the early disease stage. Krasnianski *et al.*⁸ reported a clinicopathologic analysis of 12 patients with MM2-cortical-type sCJD. Their study showed that dementia was the most frequent initial symptom; all of their patients developed dementia during the disease course. Similar to results of another study,² aphasia was common. Their patients showed apraxia more often than reported. Spatial disorientation, which is a frequent symptom of AD but not reported as typical for sCJD, was common. Their patients also showed extrapyramidal signs more often than those reported in patients with MM2-cortical-type sCJD and classic sCJD.² Again similar to results of another study,² their results indicated that the prevalence of pyramidal signs is much higher than in classic sCJD. Ataxia, which is typical in classic CJD,² was unusual. They suggested that progressive dementia with early and prominent neuropsychologic deficits in older patients should lead to suspicion of MM2-cortical-type sCJD even if other neurologic deficits are absent.⁸

The histopathologic hallmark of MM2-cortical-type sCJD is the presence of large confluent vacuole-type spongiform change,^{2,3} identified as status spongiosus by some authors,^{9,16} and more recently as coarse spongiosis.⁴ The vacuoles are several times larger than the fine vacuoles of MM1-type sCJD and are widespread in the cerebral neocortex, basal ganglia and thalamus.³ They are confluent and result in the formation of rounded islands of tissue surrounded by vacuoles reminiscent of the florid plaques of variant CJD but with the substantial difference that PrP amyloid plaques are absent.³ The distribution profile of the lesion of MM2-cortical-type sCJD is similar to that of MM1-type sCJD except in the cerebellum,^{2,3} which explains the high occurrence of neuropsychologic symptoms in MM2-cortical-type sCJD.^{2,8,10} The major neocortical lesion varies among patients.^{2,8–10} In the present patient, perivacuolar-type PrP deposition was predominant in the moderately involved occipital and temporal cortices, whereas irregular plaque-like PrP deposition was predominant in the slightly involved frontal and parietal cortices. The formation and localized accumulation of abnormal PrP is considered to be a primary pathologic event in early stage sCJD.^{1,13} Results of the present case indicate that irregular plaque-like PrP deposition occurs in the early stage of MM2-type sCJD and that perivacuolar-type PrP deposition occurs later. We believe the present patient showed early stage cerebral cortical pathology, providing a clue to the pathologic progression of this rare sCJD subtype. According to the results obtained from the present case, we suppose that the development of MM2-

cortical-type sCJD pathology, particularly of neocortical lesions, occurs as follows: (i) irregular plaque-like PrP deposition without spongiform change; (ii) large confluent vacuole-type spongiform change with perivacuolar-type PrP deposition; (iii) hypertrophic astrocytosis; and (iv) neuronal loss with tissue rarefaction. However, a detailed neuropathologic study of MM2-cortical-type sCJD by Nozaki *et al.*⁹ reported immunohistochemical findings different from ours; they reported only perivacuolar-type PrP deposition throughout the cerebral and subcortical areas. We cannot draw any conclusions regarding typical MM2-cortical-type sCJD because the present case was atypical. Further study is needed to compare the findings in this case with those of typical MM2-cortical-type sCJD.

The mechanisms underlying the two different clinicopathologic subtypes of MM2-type sCJD remain to be determined. In the present patient, the medial thalamus and inferior olivary nucleus, which are severely affected in MM2-thalamic-type sCJD,^{1,2} were relatively preserved. We believe that this neuropathologic discrepancy is important. Definitive diagnosis of MM2-cortical-type sCJD requires neuropathologic examination as well as PrP gene and Western blot analyses. The possibility of MM2-cortical-type sCJD in patients with dementia and also in patients with a typical CJD disease course should be considered. Neuropathologic examination of patterns of spongiform degeneration and PrP deposition and analysis of PrP gene and PrP type should be applied not only for typical CJD patients but also for patients with atypical progressive neurologic disorders.

REFERENCES

- Iwasaki Y, Yoshida M, Hashizume Y, Kitamoto T, Sobue G. Clinicopathologic characteristics of sporadic Japanese Creutzfeldt-Jakob disease classified according to prion protein gene polymorphism and prion protein type. *Acta Neuropathol (Berl)* 2006; **112**: 561–571.
- Parchi P, Giese A, Capellari S *et al.* Classification of sporadic Creutzfeldt-Jakob disease based on molecular and phenotypic analysis of 300 subjects. *Ann Neurol* 1999; **46**: 224–233.
- Gambetti P, Kong Q, Zou W, Parchi P, Chen SG. Sporadic and familial CJD: classification and characterization. *Br Med Bull* 2003; **66**: 213–239.
- Parchi P, Castellani R, Capellari S *et al.* Molecular basis of phenotypic variability in sporadic Creutzfeldt-Jakob disease. *Ann Neurol* 1996; **39**: 767–778.
- Hirose K, Iwasaki Y, Izumi M *et al.* MM2-thalamic-type sporadic Creutzfeldt-Jakob disease with widespread neocortical pathology. *Acta Neuropathol (Berl)* 2006; **112**: 503–511.
- Alema G, Bignami A. Polioencefalopatia degenerativa subacuta del presenio con stupore acinetico e rigidita decorticata con mioclonie (varietà "mioclonica" della malattia di Jakob-Creutzfeldt). *Rivista Sperimentale Di Freniatria E Med Legale Delle Alienazioni Mentali* 1959; **83**: 1491–1623.
- Kirschbaum WR. *Jakob-Creutzfeldt Disease*. New York: Elsevier, 1968; 1–25.
- Krasnianski A, Meissner B, Schulz-Schaeffer W *et al.* Clinical features and diagnosis of the MM2 cortical subtype of sporadic Creutzfeldt-Jakob disease. *Arch Neurol* 2006; **63**: 876–880.
- Nozaki I, Hamaguchi T, Noguchi-Shinohara M *et al.* The MM2-cortical form of sporadic Creutzfeldt-Jakob disease presenting with visual disturbance. *Neurology* 2006; **67**: 531–533.
- Hamaguchi T, Kitamoto T, Sato T *et al.* Clinical diagnosis of MM2-type sporadic Creutzfeldt-Jakob disease. *Neurology* 2005; **64**: 643–648.
- Castellani RJ, Colucci M, Xie Z *et al.* Sensitivity of 14-3-3 protein test varies in subtypes of sporadic Creutzfeldt-Jakob disease. *Neurology* 2004; **63**: 436–442.
- Kitamoto T, Shin RW, Doh-ura K *et al.* Abnormal isoform of prion proteins accumulates in the synaptic structures of the central nervous system in patients with Creutzfeldt-Jakob disease. *Am J Pathol* 1992; **140**: 1285–1294.
- Iwasaki Y, Hashizume Y, Yoshida M, Kitamoto T, Sobue G. Neuropathologic characteristics of brainstem lesions in sporadic Creutzfeldt-Jakob disease. *Acta Neuropathol (Berl)* 2005; **109**: 557–566.
- Budka H, Aguzzi A, Brown P *et al.* Neuropathological diagnostic criteria for Creutzfeldt-Jakob disease (CJD) and other human spongiform encephalopathies (prion diseases). *Brain Pathol* 1995; **5**: 459–466.
- Shiga Y, Miyazawa K, Sato S *et al.* Diffusion-weighted MRI abnormalities as an early diagnostic marker for Creutzfeldt-Jakob disease. *Neurology* 2004; **63**: 443–449.
- Masters CL, Richardson EP Jr. Subacute spongiform encephalopathy (Creutzfeldt-Jakob disease). The nature and progression of spongiform change. *Brain* 1978; **101**: 333–344.

Case Report

Coexistence of Creutzfeldt-Jakob disease, Lewy body disease, and Alzheimer's disease pathology: An autopsy case showing typical clinical features of Creutzfeldt-Jakob disease

Takashi Haraguchi¹, Seishi Terada², Hideki Ishizu³, Kenichi Sakai¹, Yasuyuki Tanabe¹, Taiji Nagai¹, Hiroshi Takata¹, Keigo Nobukuni¹, Yuetsu Ihara¹, Tetsuyuki Kitamoto⁴, Shigetoshi Kuroda²

¹Department of Neurology, National Hospital Organization Minami-Okayama Medical Center, Hayashima-cho, Tsukubo-gun, Okayama, ²Department of Neuropsychiatry, Okayama University Graduate School of Medicine, Dentistry and Pharmaceutical Sciences, Shikata-cho, Okayama, ³Department of Laboratory and Medicine, Zikei Institute, Urayasuhon-cho, Okayama, and ⁴Division of CJD Science and Technology, Department of Prion Research, Center for Translational and Advanced Animal Research on Human Diseases, Tohoku University Graduate School of Medicine, Seiryu-cho, Sendai, Japan

We report here an autopsy case of sporadic Creutzfeldt-Jakob disease (CJD) without hereditary burden and with a clinical course typical of sporadic CJD. A 77-year old man developed memory disturbance, followed by gait disturbance and myoclonus. He died of bronchopneumonia 5 months after the disease onset. Post-mortem examination revealed neuronal loss, astrocytosis, and patchy spongiosis in the cerebral cortex and lenticular nuclei. Synaptic-type deposits of prion protein were present in the cerebral cortex. Additionally, Lewy bodies were observed in the cerebral cortex and substantia nigra. Furthermore, senile plaques compatible with definite Alzheimer's disease according to Consortium to Establish a Registry for Alzheimer's disease criteria and neurofibrillary changes of the limbic system consistent with Braak stage IV were found. Based on a review of the published literature, this autopsy case is very rare, and we suppose that the incidence of CJD accompanied by Lewy body disease and Alzheimer's disease is very low.

Key words: Alzheimer's disease, Creutzfeldt-Jakob disease, Lewy body disease, neurofibrillary change, senile plaque.

INTRODUCTION

Creutzfeldt-Jakob disease (CJD) is a fatal neurodegenerative condition affecting humans and a wide variety of animals. Most cases of CJD are sporadic, arising for no obvious reason. The incidence is approximately one case per million population per year.¹⁻³ The typical clinical picture of sporadic CJD is a rapidly progressive cognitive decline with ataxia and myoclonus, associated with pseudo-periodic synchronous discharges (PSD) on the electroencephalogram and a positive CSF 14-3-3 protein test.^{1,2} The disease is neuropathologically characterized by spongiform degeneration, neuronal loss, gliosis, and the presence of altered forms of prion protein.²

Dementia with Lewy bodies (DLB) is a clinicopathological entity characterized by progressive dementia, fluctuating cognition, visual hallucination, and parkinsonism.^{4,5} The pathological features include a variable burden of α -synuclein immunoreactive neuronal pathology.^{4,5} DLB is now recognized to be the second most common cause of degenerative dementia after Alzheimer's disease (AD).⁶

The coexistence of the pathological features of CJD and AD in the same patient has rarely been demonstrated.⁷⁻¹⁰ Furthermore, senile plaques have been found at a lower frequency in sporadic CJD than in older non-demented controls.^{11,12}

In this report, we document an autopsy case with coexisting sporadic CJD, Lewy body disease (LBD), and AD pathology, in which the clinical features were those of

Correspondence: Takashi Haraguchi, MD, PhD, Department of Neurology, National Hospital Organization Minami-Okayama Medical Center, 4066 Hayashima-cho, 701-0304 Tsukubo-gun Okayama, Japan. Email: haraguchit@s-okayama.hosp.go.jp

Received 16 June 2008; revised and accepted 22 July 2008.



Fig. 1 Cranial MRI (axial, diffusion-weighted image) showing high signal intensity lesions in the temporal lobe, frontal lobe, parietal lobe cortex, and caudate nucleus (R, right side).

sporadic CJD. We also review previously reported cases of CJD accompanied by LBD or AD pathology.

CASE REPORT

Clinical course

The patient was a Japanese man who was 77 years old at the time of death. He had neither a family history of neurological disease nor dementing disorder anamnesis.

He developed memory impairment and visual disturbance in August 2003. Approximately 1 month later, he was not able to accomplish office work. He could hardly speak and became restless at night approximately 2 months after onset. His mental deterioration progressed rapidly, and he could neither stand nor walk, even with help, approximately 10 weeks after the disease onset. At admission, neurological examination revealed disorientation, confusion, and rigospasticity in the upper and lower extremities. His arms flexed at the elbows, and his legs were held in extension. Myoclonus of his face and limbs was remarkable. An EEG showed diffuse slow waves with periodic synchronous discharges (PSD). Head MRI (diffusion-weighted imaging) revealed high intensity areas in the temporal lobe, frontal lobe, parietal lobe cortex, and caudate nucleus (Fig. 1). He developed akinetic mutism approximately 3 months after the disease onset. The patient was clinically diagnosed as having CJD. He died of pneumonia approximately 5 months after the disease onset. The autopsy was limited to the brain.

Neuropathological findings

The fixed brain weighed 1220 g. Macroscopic examination revealed no significant cerebral atrophy. Meninges and vessels were normal. No pallor was noted in the substantia nigra.

The brain was fixed in 10% buffered formalin. Tissue blocks were taken from the mid-frontal and orbitofrontal areas; superior, middle and inferior temporal, inferior parietal, and occipital cortices; anterior cingulate; amygdala;

hippocampus; striatum; thalamus; midbrain; pons; medulla; and cerebellum. Multiple paraffin-embedded tissue blocks were prepared, and 6- μ m-thick sections were cut. These sections were stained with HE, KB, Bodian, methenamine silver, and Gallyas-Braak methods.

An immunocytochemical study was performed with anti- α -synuclein (C-20, a goat polyclonal antibody against the C terminus of human α -synuclein, 1:100; Santa Cruz, CA, USA). Deparaffinized sections were incubated with 1% H_2O_2 in methanol for 30 min to eliminate endogenous peroxidase activity in the tissue and treated with formic acid (99%, 5 min; Sigma, St. Louis, MO, USA) to retrieve immunogenicity. After blocking with 10% normal serum, sections were incubated overnight at 4°C with the primary antibody. The sections were washed in PBS and incubated with a biotinylated secondary antibody, followed by avidin-biotinylated horseradish peroxidase complex (ABC Elite kit, Vector, Burlingame, CA, USA). The reaction was visualized with 0.2% 3'-diaminobenzidine in 50 mmol TRIS-HCL buffer, pH 7.4, containing 0.003% H_2O_2 . Counterstaining was carried out with hematoxylin.

Microscopic examination showed neuronal loss, astrogliosis, and patchy spongiosis in the cerebral cortex (Fig. 2A) and lenticular nuclei (Fig. 2B). In the substantia nigra, neuronal loss was mild. α -Synuclein immunoreactive neurites were present in the hippocampal CA2-3 regions (Fig. 2C). Lewy bodies, which appeared as round concentric structures, were frequently observed in the cerebral cortex (Fig. 2D), amygdala, substantia nigra (Fig. 2E), locus ceruleus, and dorsal motor nucleus of the vagal nerve. The diagnosis of LBD was made on the basis of the regional density of LB, according to the pathological diagnostic criteria described in the third report of the DLB Consortium⁵: Stage 3 (four or more LB and scattered Lewy neurites (LN) per low-power field) in the temporal cortex, hippocampus, transentorhinal cortex, amygdala, substantia nigra, locus ceruleus; Stage 2 (more than one LB per low power field and sparse LN) in the cingulate; Stage 1 (sparse LB or LN) in the frontal cortex; and Stage 0 (no LB or LN)

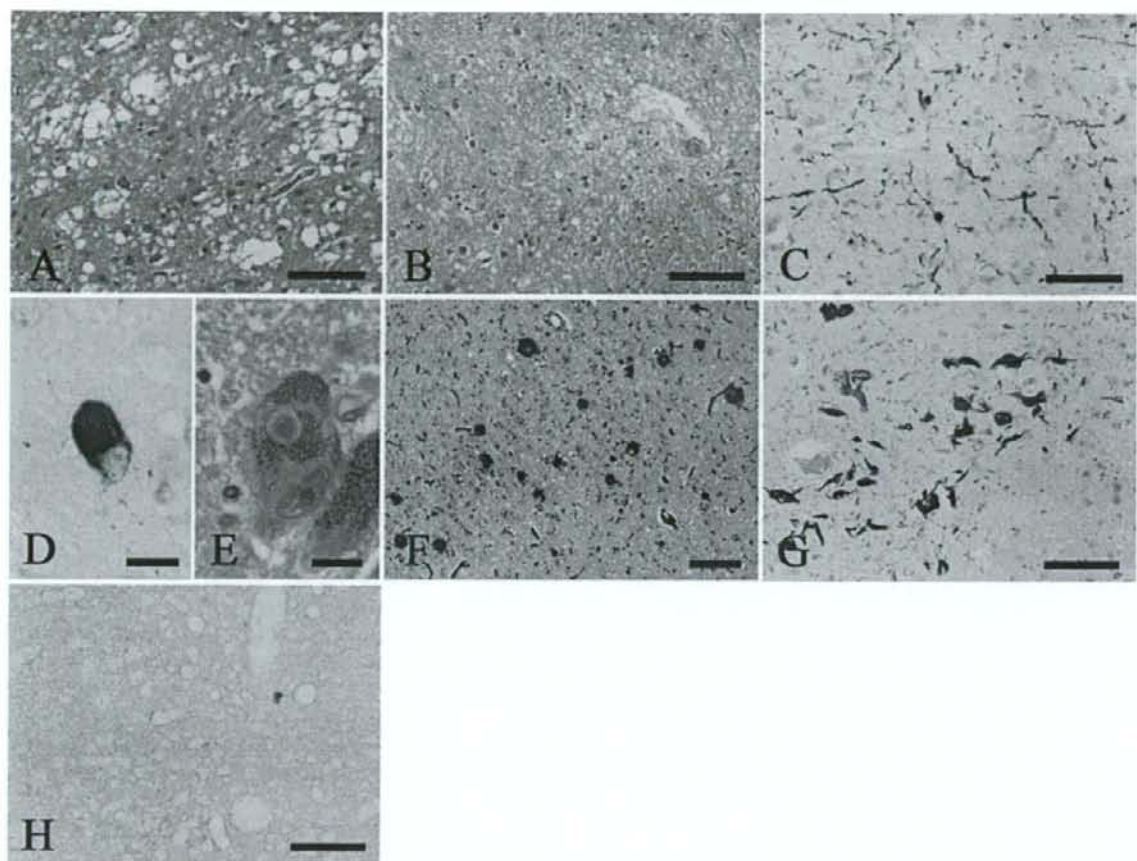


Fig. 2 Microscopic appearance of representative lesions. (A) The cerebral neocortex shows widespread status spongiosus with astrocytosis. Parietal lobe. HE. (B) The striatum also shows status spongiosus. Putamen. HE. (C) Lewy neurites are present in the hippocampus. Lewy bodies are present in the cerebral cortex (D) and substantia nigra (E). (C, D) α -Synuclein immunostaining. (E) HE stain. (F) The temporal cortex shows many senile plaques, compatible with frequent plaques of the CERAD classification. Methenamine silver stain. (G) The CA1 of the hippocampus shows a moderate number of neurofibrillary tangles. Gallyas-Braak stain. (H) The cerebral neocortex shows widespread synaptic-type prion protein (PrP) deposition. Temporal lobe. PrP immunostaining. Scale bar = (A) 100 μ m, (B) 100 μ m, (C) 50 μ m, (D) 10 μ m, (E) 10 μ m, (F) 100 μ m, (G) 100 μ m, (H) 100 μ m.

in the parietal cortex. This case corresponded to the limbic type of DLB according to the pathological diagnostic criteria of DLB.⁵

Many senile plaques were found in all isocortical-associated areas (Fig. 2F), compatible with definite AD according to Consortium to Establish a Registry for Alzheimer's Disease (CERAD) criteria.^{13,14} A modified Gallyas-Braak stain demonstrated a moderate number of neurofibrillary changes and neuropil threads in the CA1-4 and parahippocampal gyrus, consistent with stage IV of Braak's classification (Fig. 2G).

PrP studies and 14-3-3 protein study

Immunohistochemical analysis with a monoclonal antibody to prion protein (PrP) (clone 3F4; Senetec, Maryland

Heights, MO, USA) demonstrated diffuse fine granular PrP deposition (so-called synaptic-type deposition) in the cerebral cortex (Fig. 2H). PrP deposits were frequently accumulated at the periphery of senile plaques in the cerebral cortex. PrP gene analysis of frozen tissue from the cerebrum disclosed no mutations in the PrP gene open reading frame. However, polymorphic codons showed methionine homozygosity at codon 129 and glutamic acid homozygosity at codon 219. Western blotting to detect protease K-resistant PrP, performed with 3F4 in homogenized samples from the frontal and occipital lobes, disclosed protease-resistant PrP (PrP^{Sc}) type 1, according to the classification of Parchi *et al.*¹⁵ Frozen CSF obtained antemortem showed an elevation of 14-3-3 protein. We diagnosed the patient with sporadic CJD (MM1).

DISCUSSION

The diagnosis of CJD in this case was established by PrP immunostaining and Western blot analysis. We analyzed the PrP type in only two frozen cerebral cortex samples in the present case. The Western blot analysis disclosed PrP type 1, but large, confluent, spongiform vacuoles, which are characteristic of MM2-cortical-type sporadic CJD, were observed in part of the parietal cortex. Thus, the possibility of the coexistence of type 1 and type 2 PrP in the present case cannot be ruled out. The other major pathological characteristics of our patient were the presence of diffuse LB and Alzheimer pathology, including senile plaques, compatible with definite AD according to CERAD criteria, as well as neurofibrillary tangles (NFT) consistent with stage IV of Braak's classification.^{13,14,16}

The coexistence of Alzheimer pathology and prion pathology is uncommon.^{8,9,12,17,18} There are few reports of the frequency of AD pathology combined with CJD. In 1998, Hainfellner *et al.* investigated Alzheimer-type pathology according to CERAD criteria in the neocortices of 110 neuropathologically-proven CJD patients and 110 non-demented control patients and noted that Alzheimer-type pathology compatible with definite and probable AD according to CERAD criteria occurred in 10.9% of the CJD patients and 19.1% of non-demented control patients. In 12 cases of CJD with definite or probable AD according to CERAD criteria, they found a moderate frequency of NFT in only one patient, who died at 82 after a clinical duration of 3 months.¹² In 1994, Brown *et al.* presented a synopsis of the clinical, neuropathological, and biological details of a National Institutes of Health series of 189 CJD cases autopsied during the past 30 years, but only four of them were found to exhibit evidence of AD, with senile plaques and numerous NFT in the hippocampus and cerebral cortex.¹¹ In 2004, Tsuchiya *et al.* reported an autopsy case of CJD.¹⁸ The patient was a 70-year-old Japanese woman, who presented with gait disturbance as the initial sign, followed by memory impairment, visual disturbance, and myoclonus. She died of bronchopneumonia 25 months after the disease onset. The brain weighed 560 g. Histological examination revealed not only end-stage CJD, the panencephalic type, but also Alzheimer's pathology, including senile plaques compatible with definite AD according to CERAD criteria, and neurofibrillary changes of the limbic system consistent with stage IV of Braak's classification. Furthermore, from a review of the published literature, they found that the coexistence of pathological features of CJD and AD in the same patient occurs in a very small number of patients, and that there are two forms of coexistence of CJD and AD in the same patient. The first form is AD cases developing CJD in the late stage of AD.⁸⁻¹⁰ The second form is sporadic CJD cases having AD

pathological features without any clinical features typical of AD.^{7,17,19-22} Our case corresponds to the second form.

As far as we know, only three cases of CJD with LB have previously been described in detail.²³⁻²⁵ The clinical and pathological features of the autopsied CJD patients with LB, including our case, are summarized in Table 1. No case had a family history or extrinsic risk factors such as use of cadaveric human growth hormone or a dura mater graft (manufactured before the mid-1980s). The ages at onset were 64-77 years old, and the durations were 5 months to 4 years. Only our case had a clinical diagnosis of CJD in the early period of illness. The other three cases were clinically diagnosed with AD, Parkinson disease, or mood disorder. Those three cases showed parkinsonism, and the duration of the disease was more than 3 years. Because the duration of the illness in most sporadic CJD cases is less than 2 years,³ it seems legitimate to speculate that the initial symptoms resulted from Alzheimer and α -synuclein-related pathologies. Our case showed neither dementia nor parkinsonism before the clinical symptoms of CJD had clearly developed. Therefore, the clinical diagnosis of neither LBD nor AD was established ante-mortem. Two cases showed methionine/valine heterozygosity at codon 129 in the PrP gene.^{23,25} CJD with valine at the polymorphic codon 129 of the PrP gene is known to manifest different clinical and pathological features, such as a longer clinical course and plaque-type PrP deposition, from CJD with codon 129 methionine homozygosity.^{26,27} However, there has been no report of an abnormality of the PrP genes that is associated with both CJD and LBD. All three cases, including our case, in which the PrP gene was examined presented no mutation.^{23,25} Therefore, it seems reasonable to speculate that the coexistence of CJD and LBD was incidental. As shown in Table 1, brain weights were 485-1228 g. In all four cases, LB were found in the substantia nigra. In two of the four cases, cortical LB, neurofibrillary changes, and senile plaques coexisted. These two cases showed no clinical features typical of AD. From a perusal of the published literature regarding the coexistence of pathological features of CJD, LBD, and AD in the same patient, it is obvious that this case is very rare. Specifically, only two cases, including our case, have been reported.²⁵

On the other hand, the majority of DLB cases have some degree of AD pathology.^{28,29} Furthermore, in 2007, Yokota *et al.* presented the clinicopathological characteristics of two autopsy cases with both AD and DLB, possibly diagnosed as having an LB variant of AD (LBV/AD). They suggested the possibility that the propagation of Lewy-related pathology may be influenced by concurrent AD pathology, and that Lewy-related pathology could occur in the amygdala prior to the brainstem in LBV/AD. The formation of Lewy-related pathology in the amygdala may be

Table 1 Previous cases of autopsied Creutzfeldt-Jakob disease with Lewy bodies

	Iida <i>et al.</i> ²³	Ezrin-Waters <i>et al.</i> ²⁴	Vital <i>et al.</i> ²⁵	Present case
<i>Clinical features</i>				
Sex	Female	Female	Male	Male
Age at onset (years)	64	68	76	77
Age at death (years)	69	71	79	77
Duration (years)	4	3	3	0.4
Onset symptoms	Insomnia Restlessness	Akinesia Tremor	Mood change	Memory disturbance
Symptoms before clinical diagnosis of CJD				
Dementia	+	-	+	-
Parkinsonism	+	+	+	-
Initial diagnosis	AD	PD	Mood disorder	CJD
PSD	+	+	+	+
CSF 14-3-3	+	n.d.	+	+
PrP gene	Codon 129 MV Codon 219 GG	n.d.	Codon 129 MV	Codon 129 MM Codon 219 GG
PrP Western blot	n.d.	n.d.	Type 1	Type 1
<i>Histopathological features</i>				
Brain weight (g)	485	n.d.	1228	1220
Lewy body				
Cerebral cortex	-	n.d.	+	+
Substantia nigra	+	+	+	+
Lewy neurite	+	n.d.	n.d.	+
Neurofibrillary changes	n.d.	n.d.	Braak stage V	Braak stage IV
Senile plaques	n.d.	n.d.	Braak stage C	Braak stage B

-, absent; +, present; AD, Alzheimer's disease; CJD, Creutzfeldt-Jakob disease; GG, glutamine/glutamine; MM, methionine/methionine; MV, methionine/valine; n.d., not described; PD, Parkinson disease; PrP, prion protein; PSD, periodic synchronous discharges.

accelerated by tau aggregation, which also develops preferentially in the same site.³⁰ These findings, together with our study, might support the possibility that Lewy-related pathology in the brain is due to factors that are incompatible with PrP morphogenesis, in contrast with tau aggregation. However, further clinicopathological and genetic studies of similar cases will be necessary to characterize this disease entity fully and determine its etiopathology.

ACKNOWLEDGMENTS

We would like to thank Ms. M. Onbe (Department of Neuropsychiatry, Okayama University Graduate School of Medicine and Dentistry) for her excellent technical assistance. Brain tissues were obtained from the Research Resource Network, which is supported by a Research Grant for Neurological and Mental Disorders from the Ministry of Health, Labour and Welfare, Japan.

REFERENCES

- Prusiner SB. Genetic and infectious prion diseases. *Arch Neurol* 1993; **50**: 1129-1153.
- DeArmond SJ, Kretschmar HA, Prusiner SB. Prion disease. In: Graham DI, Lantos PL, eds. *Greenfield's Neuropathology*, 7th edn. London: Arnold, 2002; 273-323.
- Budka H, Parchi P, Head MK *et al.* Sporadic Creutzfeldt-Jakob disease. In: Dickson D, ed. *Pathology & Genetics: Neurodegenerative Diseases*. Basel: ISN Neuropath Press, 2003; 287-297.
- McKeith IG, Galasko D, Kosaka K *et al.* Consensus guidelines for the clinical and pathologic diagnosis of dementia with Lewy bodies (DLB): report of the consortium on DLB international workshop. *Neurology* 1996; **47**: 1113-1124.
- McKeith IG, Dickson DW, Lowe J *et al.* Diagnosis and management of dementia with Lewy bodies: third report of the DLB Consortium. *Neurology* 2005; **65**: 1863-1872.
- Lippa CF, Smith TW, Swearer JM. Alzheimer's disease and Lewy body disease: a comparative clinicopathological study. *Ann Neurol* 1994; **35**: 81-88.
- Gaches J, Supino-Viterbo V, Foncin JF. Association of Alzheimer's disease and Creutzfeldt-Jakob's disease. *Acta Neurol Belg* 1977; **77**: 202-212.
- Muramoto T, Kitamoto T, Koga H, Tateishi J. The coexistence of Alzheimer's disease and Creutzfeldt-Jakob disease in a patient with dementia of long duration. *Acta Neuropathol (Berl)* 1992; **84**: 686-689.
- Wakabayashi K, Hinokura K, Takahashi H, Seki K, Tanaka M, Ikuta F. Coexistence of Creutzfeldt-Jakob disease and senile dementia of the Alzheimer type. *Neuropathology* 1995; **15**: 122-126.

10. Brown P, Jannotta F, Gibbs CJ Jr, Baron H, Guiry DC, Gajdusek DC. Coexistence of Creutzfeldt-Jakob disease and Alzheimer's disease in the same patient. *Neurology* 1990; **40**: 226-228.
11. Brown P, Gibbs CJ Jr, Rodgers-Johnson P et al. Human spongiform encephalopathy: the National Institutes of Health series of 300 cases of experimentally transmitted disease. *Ann Neurol* 1994; **35**: 513-529.
12. Hainfellner JA, Wanschitz J, Jellinger K, Liberski PP, Gullotta F, Budka H. Coexistence of Alzheimer-type neuropathology in Creutzfeldt-Jakob disease. *Acta Neuropathol (Berl)* 1998; **96**: 116-122.
13. Hyman BT, Trojanowski JQ. Consensus recommendations for the postmortem diagnosis of Alzheimer disease from the National Institute on Aging and the Reagan Institute Working Group on diagnostic criteria for the neuropathological assessment of Alzheimer disease. *J Neuropathol Exp Neurol* 1997; **56**: 1095-1097.
14. Mirra SS, Heyman A, McKeel D et al. The Consortium to Establish a Registry for Alzheimer's Disease (CERAD). Part II. Standardization of the neuropathologic assessment of Alzheimer's disease. *Neurology* 1991; **41**: 479-486.
15. Parchi P, Castellani R, Capellari S et al. Molecular basis of phenotypic variability in sporadic Creutzfeldt-Jakob disease. *Ann Neurol* 1996; **39**: 767-778.
16. Braak H, Braak E. Neuropathological staging of Alzheimer-related changes. *Acta Neuropathol (Berl)* 1991; **82**: 239-259.
17. Powers JM, Liu Y, Hair LS, Kascsak RJ, Lewis LD, Levy LA. Concomitant Creutzfeldt-Jakob and Alzheimer diseases. *Acta Neuropathol (Berl)* 1991; **83**: 95-98.
18. Tsuchiya K, Yagishita S, Ikeda K et al. Coexistence of CJD and Alzheimer's disease: an autopsy case showing typical clinical features of CJD. *Neuropathology* 2004; **24**: 46-55.
19. Amyot R, Gauthier C. Sur la maladie de Creutzfeldt Jakob. Deux observations anatomo-cliniques. Conception uniciste. *Rev Neurol (Paris)* 1964; **110**: 473-488.
20. Hirano A, Ghatak NR, Johnson AB, Partnow MJ, Gomori AJ. Argentophilic plaques in Creutzfeldt-Jakob disease. *Arch Neurol* 1972; **26**: 530-542.
21. Horoupian DS, Ross RT. Cucumber shaped and 35 nm particles in Creutzfeldt-Jakob disease. *Can J Neurol Sci* 1975; **2**: 203-207.
22. Liberski PP, Papierz W, Alwasiak J. Creutzfeldt-Jakob disease with plaques and paired helical filaments. *Acta Neurol Scand* 1987; **76**: 428-432.
23. Iida T, Doh-ura K, Kawashima T, Abe H, Iwaki T. An atypical case of sporadic Creutzfeldt-Jakob disease with Parkinson's disease. *Neuropathology* 2001; **21**: 294-297.
24. Ezrin-Waters C, Resch L, Lang AE. Coexistence of idiopathic Parkinson's disease and Creutzfeldt-Jakob disease. *Can J Neurol Sci* 1985; **12**: 272-273.
25. Vital A, Canron MH, Gil R, Hauw JJ, Vital C. A sporadic case of Creutzfeldt-Jakob disease with beta-amyloid deposits and alpha-synuclein inclusions. *Neuropathology* 2007; **27**: 273-277.
26. Doh-ura K, Kitamoto T, Sakaki Y, Tateishi J. CJD discrepancy. *Nature* 1991; **353**: 801-802.
27. Miyazono M, Kitamoto T, Doh-ura K, Iwaki T, Tateishi J. Creutzfeldt-Jakob disease with codon 129 polymorphism (valine): a comparative study of patients with codon 102 point mutation or without mutations. *Acta Neuropathol (Berl)* 1992; **84**: 349-354.
28. Kosaka K. Diffuse Lewy body disease in Japan. *J Neurol* 1990; **237**: 197-204.
29. Kosaka K. Diffuse Lewy body disease. *Neuropathology* 2000; **20** (Suppl): 21-35.
30. Yokota O, Tsuchiya K, Uchihara T et al. Lewy body variant of Alzheimer's disease or cerebral type Lewy body disease? Two autopsy cases of presenile onset with minimal involvement of the brainstem. *Neuropathology* 2007; **27**: 21-35.

Plaque-type deposition of prion protein in the damaged white matter of sporadic Creutzfeldt-Jakob disease MM1 patients

Atsushi Kobayashi · Kunimasa Arima ·
Masafumi Ogawa · Miho Murata · Takahiro Fukuda ·
Tetsuyuki Kitamoto

Received: 29 July 2008 / Revised: 20 August 2008 / Accepted: 20 August 2008 / Published online: 28 August 2008
© Springer-Verlag 2008

Abstract Plaque-type deposition of prion protein (PrP) in the brain has been extremely rare in sporadic Creutzfeldt-Jakob disease patients with methionine homozygosity at polymorphic codon 129 of the PrP gene and type 1 abnormal isoform of PrP (sCJD-MM1). Here we report three sCJD-MM1 patients who showed prominent PrP-positive amyloid plaques in the cerebral and cerebellar white matter. All three patients showed clinical courses of long duration (2 years \leq), particularly at the end-stage. The white matter of these patients was severely damaged because of the prolonged disease duration. Furthermore, Alzheimer's amyloid precursor protein, which accumulates within the axonal swellings under pathological conditions, co-accumulated with the PrP-amyloid plaques. These findings suggest that the axonal damage reflecting the prolonged disease dura-

tion causes the deposition of PrP-amyloid plaques in the white matter. The present study shows that PrP-amyloid plaques can occur in the white matter of sCJD-MM1 cases.

Keywords Creutzfeldt-Jakob disease · Prion protein · Amyloid plaque · White matter

Introduction

The clinicopathologic phenotypes of sporadic Creutzfeldt-Jakob disease (sCJD) correlate with the genotype [methionine (M) or valine (V)] at polymorphic codon 129 of the prion protein (PrP) gene and the type (type 1 or type 2) of abnormal isoform of PrP (PrP^{Sc}) in the brain [14–16]. Type 1 and type 2 PrP^{Sc} are distinguishable according to the size of the proteinase K-resistant core of PrP^{Sc} (PrP^{res}) (21 and 19 kDa, respectively), reflecting differences in the proteinase K-cleavage site (at residues 82 and 97, respectively) [14, 17]. Based on the genotype and the PrP^{Sc} type, sCJD can be classified into six groups (MM1, MM2, MV1, MV2, VV1 and VV2) [16].

Nearly 70% of sCJD cases are classified as MM1 [16]. sCJD-MM1 is characterized by a clinical course of short duration (mean duration: 3.9 months) and synaptic-type PrP deposition in the brain [16]. However, a small subpopulation of sCJD-MM1 shows long disease duration over several years [16]. The prolonged disease duration might be due to the younger age at onset [18], or to the intensive care of the patients [5], since a comprehensive study revealed no significant difference in the physicochemical properties of PrP^{Sc} between the sCJD-MM1 cases with short and long disease duration [2]. By contrast, the synaptic-type PrP deposition is a common feature of sCJD-MM1 cases. Plaque-type PrP deposition has been extremely rare in sCJD-MM1 cases [16].

A. Kobayashi · T. Kitamoto (✉)
Division of CJD Science and Technology,
Department of Prion Research,
Tohoku University Graduate School of Medicine,
2-1 Seiryō-machi, Aoba-ku, Sendai 980-8575, Japan
e-mail: kitamoto@mail.tains.tohoku.ac.jp

K. Arima
Department of Laboratory Medicine,
National Center of Neurology and Psychiatry Musashi Hospital,
4-1-1 Ogawa-higashi-machi, Kodaira 187-8511, Japan

M. Ogawa · M. Murata
Department of Neurology,
National Center of Neurology and Psychiatry Musashi Hospital,
4-1-1 Ogawa-higashi-machi, Kodaira 187-8511, Japan

T. Fukuda
Division of Neuropathology,
Department of Neuroscience, Research Center for Medical
Sciences, The Jikei University School of Medicine,
3-25-8 Nishi-Shimbashi, Minato-ku 105-8461, Japan

Table 1 Summary of the clinical features

	Patient 1	Patient 2	Patient 3
Sex	Male	Male	Female
Age at onset (years)	69	63	71
Initial symptoms	Progressive dementia Fatigue	Progressive dementia	Progressive dementia Fatigue
Myoclonus (months) ^a	5	8	3
Akinetic mutism (months) ^a	7	12 ^b	6
PSWC on EEG (months) ^a	5	– ^c	2
Duration (months)	38	24	24

^a The duration until the appearance of myoclonus, akinetic mutism, or PSWC from onset

^b The patient became bedridden 7 months after the initial symptoms

^c Only a single EEG examination was performed 2 months after the initial symptoms. EEG revealed a short burst of delta waves and slowing of background activities

Here we report three sCJD-MM1 patients with prominent PrP-positive amyloid plaques in the cerebral and cerebellar white matter. All three patients showed clinical courses of long duration. Therefore, we discuss correlations among the long disease duration, white matter involvement, and PrP-amyloid plaques.

Patients and methods

Patients

The clinical features of the three patients are summarized in Table 1 and Fig. 1. The clinical signs at onset were complaint of fatigue and progressive dementia (memory loss, disorientation and miscalculation). Electroencephalogram (EEG) showed periodic sharp wave complex (PSWC) in patients 1 and 3. In patient 2, only a single EEG examination was performed 2 months after the initial symptoms, which revealed a short burst of delta waves and slowing of background activities. The patients became bedridden 5 months (patient 1), 7 months (patient 2), or 4 months (patient 3) after the initial symptoms, and then fell into

akinetic mutism 7 months (patient 1), 12 months (patient 2), or 6 months (patient 3) after the onset. The total disease duration was 38 months (patient 1) or 24 months (patients 2 and 3). The past medical history was unremarkable with no neurological surgery, no exposure to iatrogenic CJD, and no brain trauma. There was no family history of similar disorders.

PrP gene analysis

Genomic DNA was extracted from peripheral blood leukocytes, and the coding region of the PrP gene was analyzed as previously described [7].

Western blot analysis

Brain tissues were obtained at autopsy after receiving informed consent for research use. The brains were immediately frozen or fixed in 10% buffered formalin. PrP^{Sc} was extracted from the frontal cortex with collagenase treatment as described [3] with modifications. Samples were subjected to 13.5% SDS-PAGE and western blotting as described [1]. The 3F4 monoclonal antibody (Signet Laboratories) was used as the primary antibody. Goat-anti-mouse immunoglobulin polyclonal antibody labeled with the peroxidase-conjugated dextran polymer, EnVision+ (DakoCytomation), was used as the secondary antibody.

Neuropathology

Formalin-fixed brains were treated with 99% formic acid for 1 h to inactivate the infectivity and were embedded in paraffin. Tissue sections were stained with hematoxylin and eosin (H&E) for routine neuropathological examination. For Congo red staining, tissue sections were incubated in a solution containing 1% Congo red and 50% ethanol for

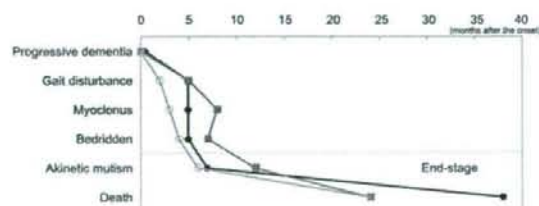


Fig. 1 The clinical courses of patient 1 (filled circle), patient 2 (filled square), and patient 3 (open circle). After the rapid exacerbation period, a prolonged end-stage followed

30 min. After washing with a solution containing 50% ethanol and 1% sodium hydroxide, the sections were counterstained with hematoxylin. For the PrP immunohistochemistry, tissue sections were pretreated by hydrolytic autoclaving [6]. The #71 monoclonal antibody was used as the primary antibody [10, 19]. Anti-mouse EnVision+ was used as the secondary antibody. For the immunohistochemical detection of the Alzheimer's amyloid precursor protein (APP), tissue sections were pretreated by hydrated autoclaving with 10 mM EDTA pH 6.0 [11, 20]. The UT-18 polyclonal antibody was used as the primary antibody [21]. Anti-rabbit EnVision+ was used as the secondary antibody. The color was developed with diaminobenzidine for single immunostaining or with diaminobenzidine and cobalt chloride [12] for double staining. For double staining with Congo red, the color-developed immunostained sections were washed with water for 5 min and then stained with Congo red as described earlier. In this paper, we term PrP deposits clearly observed on H&E-stained sections and showing green birefringence on adjacent Congo red-stained sections as (amyloid) plaques. Focal PrP-immunolabelings are generically termed as plaque-type PrP deposits, which include amyloid plaques.

Results

PrP gene analysis

All three patients were homozygous for methionine at polymorphic codon 129 (129 M/M) and for glutamic acid at polymorphic codon 219 (219E/E) of the PrP gene. There was no mutation in the coding region of the PrP gene.

Western blot analysis

Western blot analysis of the brains after proteinase-K digestion revealed that the size of PrP^{res} was identical with type 1 PrP^{res} from a typical sCJD-MM1 case (Fig. 2). Type 2 PrP^{res} was not detected.

Neuropathology

The brains weighed 680 g (patient 1), 1,000 g (patient 2), or 840 g (patient 3). The cerebral cortex was very thin, and the white matter was atrophic. On microscopic examination, severe neuronal loss and marked astrocytosis were observed in the cerebral cortex, thalamus and cerebellar cortex (Fig. 3a). The basal ganglia, hippocampus and brainstem were relatively spared. The cerebral and cerebellar white matter showed severe degeneration with the infiltration of macrophages. In patients 1 and 2, many amyloid plaques were observed in the white matter of the

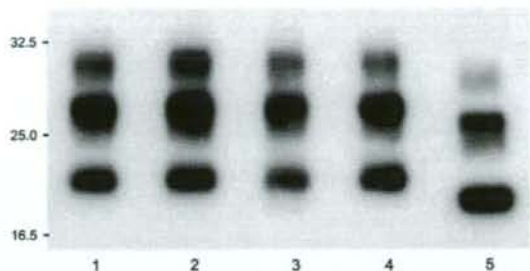


Fig. 2 Western blot analysis of PrP^{res} in the homogenates of the frontal cortex from patient 1 (lane 2), patient 2 (lane 3), or patient 3 (lane 4). The size and glycosylation pattern of PrP^{res} from the three patients were identical with type 1 PrP^{res} from a typical sCJD-MM1 case (lane 1), but different from type 2 PrP^{res} from a sCJD-MM2 case (lane 5)

cerebral cortex, parahippocampal gyrus, basal ganglia, thalamus, and cerebellar cortex (Fig. 3b). Congo red staining revealed that these amyloid plaques showed green birefringence under polarized light (Fig. 3c). Immunohistochemical analysis using anti-human PrP antibody #71 revealed numerous plaque-type PrP deposits in the white matter besides synaptic-type PrP deposition in the grey matter (Fig. 3d–f). PrP-positive plaques were prominent particularly in the parahippocampal gyrus and basal ganglia (Table 2). In patient 3, plaque-type PrP deposition in the white matter was restricted to within the parahippocampal gyrus.

To evaluate the extent of the axonal damage, we investigated the accumulation of APP in the white matter. APP accumulates within the axonal swellings of brain lesions such as those by infarction [13]. Therefore, we performed immunohistochemical analysis using anti-APP polyclonal antibody UT-18 [21]. In patients 1 and 2, there were many APP immunoreactivities in the white matter of the parahippocampal gyrus and basal ganglia (Fig. 4a). The accumulation of APP was also observed in the white matter of the frontal and temporal cortex of patient 2. APP accumulation was not observed in the brain sections from patient 3 or typical sCJD-MM1 cases with short disease duration (data not shown). Thus, the intensity and distribution of APP immunoreactivities in the white matter correlated well with those of PrP-amyloid plaques. Furthermore, some of these APP immunoreactivities were enclosed in amyloid plaque-like structures (Fig. 4b). Double staining with APP immunohistochemistry and Congo red revealed the co-localization of APP and amyloid plaques (Fig. 4c). To examine the co-accumulation of APP and PrP, we performed immunohistochemical analysis of the serial sections using anti-APP or anti-PrP antibody. A significant portion of the APP immunoreactivities was co-localized with PrP-amyloid plaques in patients 1 and 2 (Fig. 4d, e).

Fig. 3 **a** The cerebral cortex showed extensive neuronal loss and gliosis. The white matter was also severely damaged (frontal cortex of patient 2; H&E; $\times 20$). **b** Amyloid plaque in the basal ganglia (patient 2; H&E; $\times 600$). **c** Amyloid plaques in the white matter were stained with Congo red and showed green birefringence under polarized light (parahippocampal gyrus of patient 1; Congo red; $\times 200$). **d–f** Immunohistochemistry for PrP revealed numerous plaque-type PrP deposits in the white matter of the frontal cortex (**d** patient 2; #71 antibody; $\times 40$), parahippocampal gyrus (**e** patient 1; #71 antibody; $\times 200$), and basal ganglia (**f** patient 2; #71 antibody; $\times 100$)

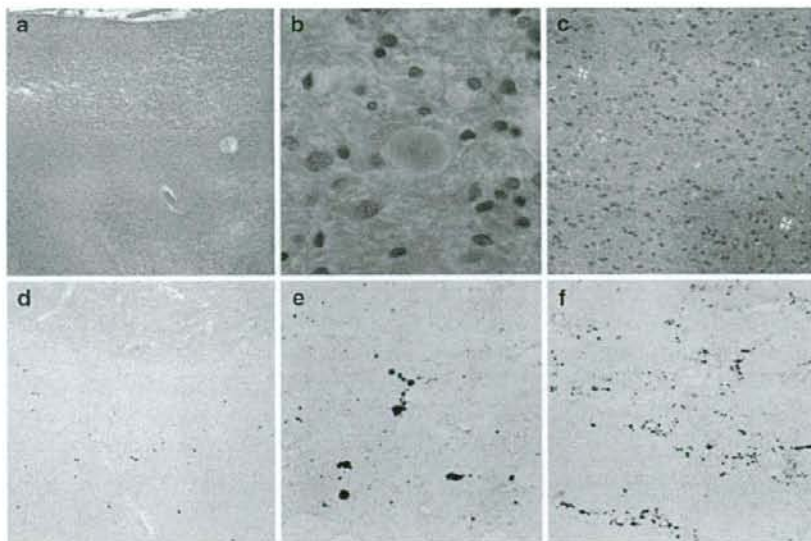


Table 2 Distribution of PrP-amyloid plaques

Patient	PrP-amyloid plaques in the white matter ^a					
	Frontal cortex	Occipital cortex	Parahippocampus	Basal ganglia	Thalamus	Cerebellum
1	+	–	+++	+++	+	++
2	+++	+	+++	+++	++	++
3	–	–	++	–	–	–

^a The sum of the number of PrP-positive plaques in 10 fields ($\times 100$ magnification)

– 0, + 1–10, ++ 11–100, +++ 100<

Discussion

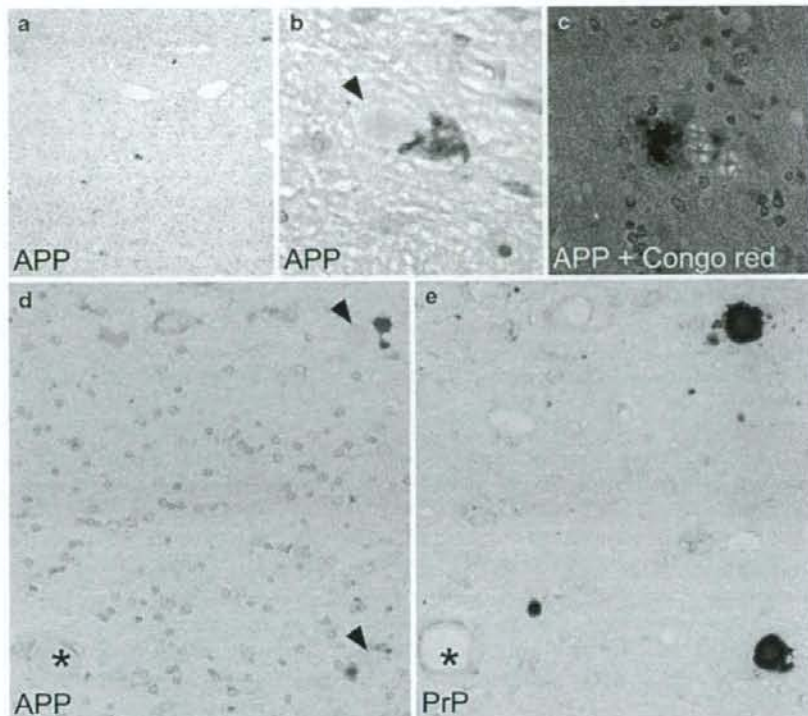
Here we report three patients with sCJD-MM1 who showed prominent PrP-positive amyloid plaques in the cerebral and cerebellar white matter. PrP-amyloid plaques have been extremely rare in sCJD-MM1 cases, but the present three patients demonstrate that this could occur.

To date, CJD cases with the 129 M/M genotype and plaque-type PrP deposits have been mainly recognized in the infectious form of CJD, e.g., variant CJD (vCJD) or iatrogenic CJD. Only a single sCJD-MM1 case with amyloid plaques has been reported [4], but this case had a history of neurosurgery. Thus, the possibility of iatrogenic transmission of CJD other than sCJD-MM1 could not be excluded. In the present study, however, none of the three patients had any history of neurosurgery or hormone therapy. Moreover, the size of PrP^{res} in the brain was identical with that of type 1 PrP^{res} from a typical sCJD-MM1 case. Type 2 PrP^{res} or the intermediate type PrP^{res} [8], which is observed in vCJD or the plaque-type of dura graft-associated CJD (p-dCJD) cases, was not detected in the brains of the three patients. In addition, PrP-amyloid plaques were restricted

within the white matter in the present cases. The distribution of the plaques differed from that observed in vCJD or p-dCJD cases. Therefore, it is certain that the three patients in this report should be classified into sCJD-MM1, but not the infectious form of CJD.

Co-accumulation of APP and PrP suggests that the axonal damage, i.e., impaired axonal transport, causes the deposition of PrP-amyloid plaques in the white matter of sCJD-MM1 cases. APP is transported by the fast anterograde component of axonal flow [9]. Under various pathological conditions, APP accumulates within the axonal swellings because of impaired axonal transport [13]. In the present study, PrP-amyloid plaques were identified exclusively in the white matter and most commonly in conjunction with APP. These findings indicate that PrP might accumulate within the axonal swellings in the damaged white matter and then form amyloid plaques. However, since plaque-type PrP deposits were more than APP deposits in all brain sections examined and APP accumulation was not observed in patient 3, we cannot rule out the reverse hypothesis that PrP-plaques in the white matter induce the axonal damage in case of long disease duration.

Fig. 4 **a** Immunohistochemistry using anti-APP antibody revealed many APP accumulations in the cerebral white matter (basal ganglia of patient 2; UT-18 antibody; $\times 100$). **b** APP immunoreactivity adjacent to amyloid plaque-like structure (*arrowhead*) (basal ganglia of patient 2, UT-18 antibody; $\times 600$). **c** Double staining with the APP immunohistochemistry and Congo red revealed co-localization of APP and amyloid plaques (basal ganglia of patient 2; UT-18 antibody and Congo red; $\times 400$). **d, e** Immunohistochemical analysis of the serial sections using anti-APP or anti-PrP antibody revealed that the APP immunoreactivities were co-localized with PrP-positive amyloid plaques (*arrowheads*) (parahippocampal gyrus of patient 1; **d** UT-18 antibody; **e** #71 antibody; $\times 400$). *Asterisk* denotes a landmark vessel to indicate the serial sections



The most plausible explanation for the axonal damage is the prolonged disease duration. The three patients in this report showed clinical courses of long duration (2 years \leq). In sCJD-MM1 cases with long disease duration, the white matter is severely affected as the end-stage pathology of CJD [2, 5]. These findings lead us to surmise that PrP-amyloid plaques in the white matter may be a common feature of sCJD-MM1 cases with prolonged disease duration. However, it has been reported that four Japanese sCJD-MM1 cases with long disease duration of over 2 years showed no plaque-type PrP deposition in the white matter [5]. Therefore, not only the disease duration but also unidentified factors such as pharmacological treatment, minor trauma, or hypoxia during the clinical course might modify the pattern of PrP deposition.

As an explanation for PrP-amyloid plaques, we cannot rule out the possible existence of different prion strains in sCJD-MM1 prions. However, the biochemical properties of PrP^{Sc} in the brain are identical between the sCJD-MM1 cases with long and short disease duration [2]. In line with these findings, the three patients in this report had type 1 PrP^{res} identical in size and glycoform ratio to that from typical sCJD-MM1 cases. In addition, in contrast to the prolonged end-stage, the exacerbation periods of the three patients were as short as those of typical sCJD-MM1 cases. Thus, it is highly unlikely that an atypical prion strain

caused PrP-amyloid plaques in the present cases. To exclude this possibility, it will be necessary to perform a transmission study using sCJD-MM1 prions from the present three patients.

In conclusion, this study shows that PrP-amyloid plaques can occur in the white matter of sCJD-MM1 cases with prolonged disease duration. Although plaque-type PrP deposition is a characteristic of other subtypes of CJD including sCJD-MV2, VV2, vCJD or p-dCJD, the plaques in the white matter of these cases might also have resulted from the axonal damage reflecting the prolonged disease duration rather than prion strain-dependent properties.

Acknowledgments We thank H. Kudo, K. Abe and M. Kimura for their technical assistance, and B. Bell for critical review of the manuscript. We are grateful to Dr. T. Suzuki for providing the UT-18 antibody. This study was supported by the Program for Promotion of Fundamental Studies in Health Sciences of National Institute of Biomedical Innovation (T.K.), a grant from the Ministry of Health, Labor and Welfare (A.K. and T.K.), and a Grant-in-Aid for Scientific Research from the Ministry of Education, Culture, Sports, Science and Technology (A.K. and T.K.).

References

- Asano M, Mohri S, Ironside JW, Ito M, Tamaoki N, Kitamoto T (2006) vCJD prion acquires altered virulence through trans-species

- infection. *Biochem Biophys Res Commun* 342:293–299. doi:10.1016/j.bbrc.2006.01.149
2. Cali L, Castellani R, Yuan J et al (2006) Classification of sporadic Creutzfeldt-Jakob disease revisited. *Brain* 129:2266–2277. doi:10.1093/brain/awl224
 3. Grathwohl KUD, Horiuchi M, Ishiguro N, Shinagawa M (1996) Improvement of PrP^{Sc}-detection in mouse spleen early at the pre-clinical stage of scrapie with collagenase-completed tissue homogenization and Sarkosyl-NaCl extraction of PrP^{Sc}. *Arch Virol* 141:1863–1874. doi:10.1007/BF01718200
 4. Ishida C, Kakishima A, Okino S et al (2003) Sporadic Creutzfeldt-Jakob disease with MM1-type prion protein and plaques. *Neurology* 60:514–517
 5. Iwasaki Y, Yoshida M, Hashizume Y, Kitamoto T, Sobue G (2006) Clinicopathologic characteristics of sporadic Japanese Creutzfeldt-Jakob disease classified according to prion protein gene polymorphism and prion protein type. *Acta Neuropathol* 112:561–571. doi:10.1007/s00401-006-0111-7
 6. Kitamoto T, Shin RW, Doh-ura K et al (1992) Abnormal isoform of prion proteins accumulates in the synaptic structures of the central nervous system in patients with Creutzfeldt-Jakob disease. *Am J Pathol* 140:1285–1294
 7. Kitamoto T, Ohta M, Doh-ura K, Hitoshi S, Terao Y, Tateishi J (1993) Novel missense variants of prion protein in Creutzfeldt-Jakob disease or Gerstmann-Sträussler syndrome. *Biochem Biophys Res Commun* 191:709–714. doi:10.1006/bbrc.1993.1275
 8. Kobayashi A, Asano M, Mohri S, Kitamoto T (2007) Cross-sequence transmission of sporadic Creutzfeldt-Jakob disease creates a new prion strain. *J Biol Chem* 282:30022–30028. doi:10.1074/jbc.M704597200
 9. Koo EH, Sisodia SS, Archer DR et al (1990) Precursor of amyloid protein in Alzheimer disease undergoes fast anterograde axonal transport. *Proc Natl Acad Sci USA* 87:1561–1565. doi:10.1073/pnas.87.4.1561
 10. Muramoto T, Tanaka T, Kitamoto N et al (2000) Analysis of Gerstmann-Sträussler syndrome with 102Leu219Lys using monoclonal antibodies that specifically detect human prion protein with 219Glu. *Neurosci Lett* 288:179–182. doi:10.1016/S0304-3940(00)01232-5
 11. Murayama H, Shin RW, Higuchi J, Shibuya S, Muramoto T, Kitamoto T (1999) Interaction of aluminum with PHF τ in Alzheimer's disease neurofibrillary degeneration evidenced by desferrioxamine-assisted chelating autoclave method. *Am J Pathol* 155:877–885
 12. Ohgami T, Kitamoto T, Shin RW, Kaneko Y, Ogomori K, Tateishi J (1991) Increased senile plaques without microglia in Alzheimer's disease. *Acta Neuropathol* 81:242–247. doi:10.1007/BF00305864
 13. Ohgami T, Kitamoto T, Tateishi J (1992) Alzheimer's amyloid precursor protein accumulates within axonal swellings in human brain lesions. *Neurosci Lett* 136:75–78. doi:10.1016/0304-3940(92)90651-M
 14. Parchi P, Castellani R, Capellari S et al (1996) Molecular basis of phenotypic variability in sporadic Creutzfeldt-Jakob disease. *Ann Neurol* 39:767–778. doi:10.1002/ana.410390613
 15. Parchi P, Capellari S, Chen SG et al (1997) Typing prion isoforms. *Nature* 386:232–233. doi:10.1038/386232a0
 16. Parchi P, Giese A, Capellari S et al (1999) Classification of sporadic Creutzfeldt-Jakob disease based on molecular and phenotypic analysis of 300 subjects. *Ann Neurol* 46:224–233. doi:10.1002/1531-8249(199908)46:2<224::AID-ANA12>3.0.CO;2-W
 17. Parchi P, Zou W, Wang W et al (2000) Genetic influence on the structural variations of the abnormal prion protein. *Proc Natl Acad Sci USA* 97:10168–10172. doi:10.1073/pnas.97.18.10168
 18. Pocchiari M, Puopolo M, Croes EA et al (2004) Predictors of survival in sporadic Creutzfeldt-Jakob disease and other human transmissible spongiform encephalopathies. *Brain* 127:2348–2359. doi:10.1093/brain/awh249
 19. Satoh K, Muramoto T, Tanaka T et al (2003) Association of an 11–12 kDa protease-resistant prion protein fragment with subtypes of dura graft-associated Creutzfeldt-Jakob disease and other prion diseases. *J Gen Virol* 84:2885–2893. doi:10.1099/vir.0.19236-0
 20. Shin RW, Iwaki T, Kitamoto T, Tateishi J (1991) Hydrated autoclave pretreatment enhances tau immunoreactivity in formalin-fixed normal and Alzheimer's disease brain tissues. *Lab Invest* 64:693–702
 21. Tomita S, Ozaki T, Taru H et al (1999) Interaction of a neuron-specific protein containing PDZ domains with Alzheimer's amyloid precursor protein. *J Biol Chem* 274:2243–2254. doi:10.1074/jbc.274.4.2243

Human Prion Protein (PrP) 219K Is Converted to PrP^{Sc} but Shows Heterozygous Inhibition in Variant Creutzfeldt-Jakob Disease Infection^{*[S]}

Received for publication, December 9, 2008; Published, JBC Papers in Press, December 10, 2008; DOI 10.1074/jbc.M809254200

Masaki Hizume^{†§1}, Atsushi Kobayashi^{†1}, Kenta Teruya[†], Hiroaki Ohashi^{||}, James W. Ironside^{**}, Shirou Mohri^{††}, and Tetsuyuki Kitamoto^{‡2}

From the [†]Division of CJD Science and Technology, [‡]Division of Prion Biology, Department of Prion Research, Tohoku University Graduate School of Medicine, Sendai 980-8575, Japan, the ^{||}Central Institute for Experimental Animals, Kawasaki 216-0011, Japan, the ^{**}National CJD Surveillance Unit, Western General Hospital, Edinburgh EH4 2XU, United Kingdom, the ^{††}Prion Disease Research Center, National Institute of Animal Health, Tsukuba 305-0856, Japan, and the [§]Department of Neurology and Neurological Science, Graduate School, Tokyo Medical and Dental University, Bunkyo-ku, Tokyo 113-8519, Japan

Prion protein gene (*PRNP*) E219K is a human polymorphism commonly occurring in Asian populations but is rarely found in patients with sporadic Creutzfeldt-Jakob disease (CJD). Thus the polymorphism E219K has been considered protective against sporadic CJD. The corresponding mouse prion protein (PrP) polymorphism variant (mouse PrP 218K) is not converted to the abnormal isoform (PrP^{Sc}) and shows a dominant negative effect on wild-type PrP conversion. To define the conversion activity of this human molecule, we herein established knock-in mice with human PrP 219K and performed a series of transmission experiments with human prions. Surprisingly, the human PrP 219K molecule was converted to PrP^{Sc} in variant CJD infection, and the conversion occurred more efficiently than PrP 219E molecule. Notably the knock-in mice with *PRNP* codon 219E/K showed the least efficient conversion compared with their hemizygotes with *PRNP* codon 219E/0 or codon 219K/0, or homozygotes with *PRNP* codon 219E/E or codon 219K/K. This phenomenon indicated heterozygous inhibition. This heterozygous inhibition was observed also in knock-in mice with *PRNP* codon 129M/V genotype. In addition to variant CJD infection, the human PrP 219K molecule is conversion-competent in transmission experiments with sporadic CJD prions. Therefore, the protective effect of *PRNP* E219K against sporadic CJD might be due to heterozygous inhibition.

Human prion diseases have been classified into infectious, inherited, and sporadic forms. Infectious human prion disease was demonstrated first in Kuru (1) and recently in Creutzfeldt-

Jakob disease (CJD)³ with dura mater-grafted CJD, pituitary hormone-associated CJD, and variant CJD (vCJD) (2, 3). Familial CJD, Gerstmann-Straussler syndrome, and fatal familial insomnia are human inherited prion diseases (4). Sporadic CJD (sCJD) is of unknown etiology. These prion diseases are caused by the accumulation of an abnormal isoform (PrP^{Sc}) of prion protein (PrP), which is converted from the normal cellular isoform (PrP^C) (5). The human PrP contains 253 amino acids encoded by prion protein gene (*PRNP*), which is located on chromosome 20. Numerous point mutations or insertional mutations in the open reading frame of *PRNP* have been reported in inherited prion diseases. In addition, normal polymorphisms of *PRNP* appear to influence the susceptibility to sporadic or infectious prion diseases. Homozygosity at the polymorphic *PRNP* codon 129 (methionine or valine) may cause a predisposition to sporadic or iatrogenic CJD in Europeans (6, 7). All cases of vCJD are homozygous for methionine at *PRNP* codon 129 (129M/M) (8).

In 1994, we reported that glutamate to lysine substitution at codon 219 is a polymorphism occurring in the Japanese population (9). This is a common polymorphism (allele frequency; 6%), which was later found also in other populations in the East Asia, the South Asian subcontinent, and the Pacific region, but has not been reported in Europeans (10–12). It has been reported that the *PRNP* genotype at codon 219 influences the clinicopathological features of Gerstmann-Straussler syndrome with a codon 102 mutation (13), and that the codon 219K genotype appears to have a protective effect for sCJD (14). In addition, the codon 218K variant (corresponding to the human 219K) in the murine prion protein gene (*prnp*) was not converted to PrP^{Sc} and also showed a dominant negative effect on wild-type PrP conversion both in scrapie-infected neuroblastoma cells (15) and in transgenic mice (16). This dominant negative effect of the mouse PrP 218K variant was proposed at first to be mediated by protein X (15) but was also observed in *in vitro* fibril formation without protein X (17). In contrast to the murine *prnp* 218K variant, the human PrP 219K molecule did

^{*} This work was supported by the Promotion of Fundamental Studies in Health Science of National Institute of Biomedical Innovation (to H. O., S. M., and T. K.), a grant from the Ministry of Health, Labor, and Welfare (to A. K., S. M., and T. K.), and a Grant-in Aid for Scientific Research from the Ministry of Education, Culture, Sports, Science and Technology (to A. K. and T. K.). The costs of publication of this article were defrayed in part by the payment of page charges. This article must therefore be hereby marked "advertisement" in accordance with 18 U.S.C. Section 1734 solely to indicate this fact.

^[S] The on-line version of this article (available at <http://www.jbc.org>) contains supplemental Figs. S1–S4.

¹ Both authors contributed equally to this work.

² To whom correspondence should be addressed: Division of CJD Science and Technology, Dept. of Prion Research, Tohoku University Graduate School of Medicine, 2-1 Seiryō, Aoba, Sendai 980-8575, Japan. Tel.: 81-22-717-8143; Fax: 81-22-717-8148; E-mail: kitamoto@mail.tains.tohoku.ac.jp.

³ The abbreviations used are: CJD, Creutzfeldt-Jakob disease; vCJD, variant CJD; sCJD, sporadic CJD; PrP, prion protein; PrP^C, normal cellular isoform of PrP; PrP^{Sc}, abnormal isoform of PrP; FDC, follicular dendritic cell; *PRNP*, human prion protein gene; *prnp*, murine prion protein gene.

Conversion and Inhibitory Effect of PrP 219K

not prevent the onset of dura mater-grafted CJD (14) or familial CJD (18). Therefore, it remains unclear whether the human PrP 219K molecule is conversion-competent or not.

In the present study, we newly established knock-in mice expressing the human PrP 219K molecule (Ki-Hu219K/K) and compared the conversion activity with other human PrP polymorphic molecules (19). We found that human PrP 219K is readily converted to PrP^{Sc} in vCJD infection, and also report the inhibition of PrP conversion in the heterozygous knock-in models.

EXPERIMENTAL PROCEDURES

Production of Humanized Knock-in Mouse with Homozygous, Heterozygous, or Hemizygous Genetic Background—Knock-in mice and transgenic mice were generated as reported previously (20). The open reading frame was replaced with human PrP gene with lysine at codon 219 (Fig. 1A). The 5'-primer was designed to incorporate a SmaI site. The PCR fragment was ligated to the mouse sequence using the SmaI site. Consequently, after processing of the N-terminal signal peptide during post-translational modification, the resulting molecule was identical with human PrP. The knock-in mice with human PrP 129M or 129V were already established (19, 21). We produced knock-in mouse crossed with the PrP knock-out mouse (20) to provide the hemizygous genetic background in the present study.

Sources of Prion Inocula and Transmission Experiment—Human brain tissues were obtained at autopsy from CJD patients after receiving informed consent for research use. Brain homogenate was prepared from four patients with vCJD (96/02, 96/07, 96/45, or 05/02), or two cases with sCJD (MM1 and MV1). The open reading frame of *PRNP* was analyzed by PCR direct sequencing (22). Human brain homogenates (10%) were prepared as described previously (23). Transmission studies were performed using 20 μ l of the homogenates for intracerebral inoculation or 50 μ l for intraperitoneal inoculation. Mice were sacrificed at 75 days post-inoculation for follicular dendritic cell (FDC) bioassay. Our previous study showed that the level of PrP^{Sc} accumulated in the spleen of knock-in mouse expressing chimeric human/mouse PrP with 129 M/M reached a plateau at 45 days post-inoculation (20). Thus, we decided to perform FDC assay at 75 days post-inoculation (19). Half of the spleen was immediately frozen for Western blotting, and the remaining half was fixed in 10% buffered formalin for the immunohistochemistry. Intracerebrally inoculated mice were sacrificed after the onset of the disease or examined when post-mortem. One hemisphere of the brain was immediately frozen for Western blotting, and the other hemisphere was fixed in formalin for the immunohistochemistry.

Immunohistochemistry—Mouse tissues were fixed with 10% buffered formalin, and treated with 60% formic acid before embedding in paraffin. Tissue sections were processed for PrP immunohistochemistry using hydrolytic autoclaving pretreatment (24). The PrP-N antiserum (25) or ChW antiserum (19) were used as the primary antibody. A goat anti-rabbit immunoglobulin polyclonal antibody labeled with a peroxidase-conjugated dextran polymer, EnVision (DakoCytomation, Denmark), was used as the secondary antibody.

Western Blotting—PrP^{Sc} was extracted from either spleen or brain with collagenase treatment as previously described (26) with modifications. PrP^C was measured in the membrane fractions of the brain isolated from the knock-in mice. For the quantitative analysis, samples (corresponding to 7.5 mg wet weight of spleen tissue for PrP^{Sc}, or 500 μ g wet weight of brain tissue for PrP^C) were subjected to 13.5% SDS-PAGE and transferred to polyvinylidene difluoride membrane. ChW antiserum or 3F4 antibody was used as the primary antibody. Anti-rabbit or anti-mouse EnVision was used as the secondary antibody. Enhanced chemiluminescence detection (GE Healthcare) was used to visualize Western blots. The signal intensities of the Western blots were quantified with Quantity One software using an imaging device, Vasa Doc 5000 (Bio-Rad). Western blot analysis was repeated at least three times, and signal intensities were expressed as mean \pm S.E.

To check the protease resistance in each PrP polymorphism, we did the following experiment with the infected or uninfected knock-in mouse brains. Brain tissues of the Ki-Hu219K/K or Ki-Hu219E/E infected with MM1 prions or the uninfected control brain tissues were homogenized with 10 times the amount of the buffer containing 50 mM Tris-HCl (pH 8.0), 150 mM NaCl, and protease inhibitors (Complete, Roche Applied Science). The homogenates were centrifuged at 1000 \times g for 10 min to discard the nuclear fraction. The supernatants were homogenized again with a glass homogenizer adding the Sarkosyl solution at a final concentration of 2%. The homogenate was centrifuged again at 2000 \times g for 10 min. The final supernatant was digested at 37°C for 60 min with Proteinase K at concentrations of 0, 1, 3, 10, 30, 100, and 300 μ g/ml. The digested samples were added with the equal volume of Laemmli sample buffer and boiled for 15 min for the Western blot analysis.

Statistical Analysis—Incubation times and the signal intensities of Western blots are expressed as mean \pm S.E.

RESULTS

Knock-in Mouse as a Model to Provide the Physiological Expression Level of Recombinant PrP—In comparison with transgenic technology, knock-in mice produced by the homologous recombination technique have the advantage of providing a constant expression level (20, 27). Therefore, as reported previously (19), the expression level of PrP^C in the spleens of the heterozygous knock-in mice (Ki-Hu129M/V) was the same as that of the homozygous knock-in mice (Ki-Hu129M/M or Ki-Hu129V/V). It is impossible to establish a heterozygous animal model without the homologous recombination technique. However, a transgenic model with the *PRNP* 129M/V genotype was reported previously, but this model (Tg45/152) showed uneven expression (M:V = 1:1.5) and overexpression of the gene (4–6 fold) (28). In addition to the advantage described above, here we present that the expression levels of PrP^C in the brains of the hemizygous knock-in mice (Ki-Hu129M/0 or Ki-Hu129V/0) showed almost half the intensities of those seen in the homozygous mice (Ki-Hu129M/M or Ki-Hu129V/V) (Fig. 1, B and C). Thus, in this study, we can analyze two different expression levels of recombinant PrP: 1 copy of gene expression in the hemizygous knock-in mice and 2 copies of

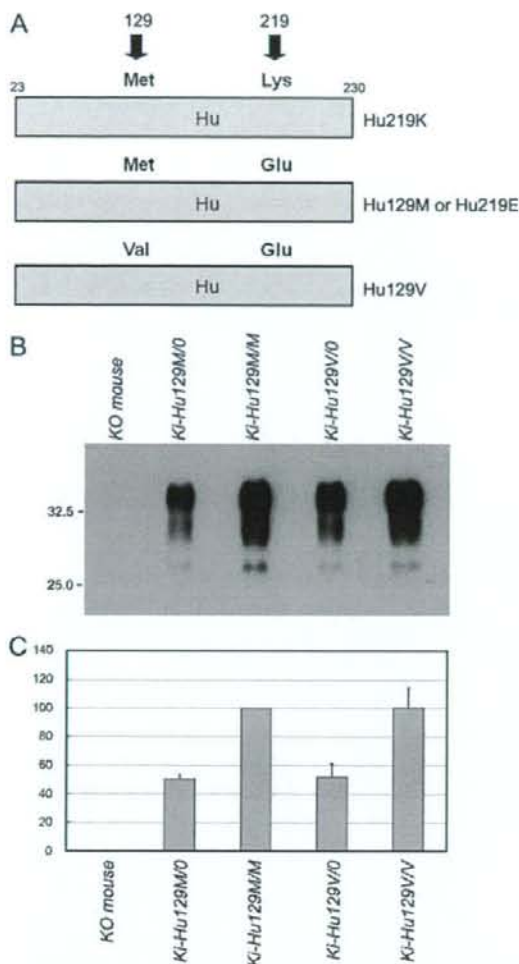


FIGURE 1. Characterization of the knock-in mice. *A*, the open reading frames of the knock-in vectors. The Hu219K vector encodes methionine at codon 129 and lysine at codon 219. The Hu219M (a synonym for Hu219E) and the Hu219V vectors were reported previously (19). *B*, Western blot analysis of the membrane fraction of the brains from the knock-out mouse, the hemizygous knock-in mice, and the homozygous knock-in mice. The position of molecular size standards is shown on the left (kilodaltons). *C*, the comparatively corrected signal intensities (numbers/mm²) are presented. We assigned a signal intensity of 100/mm² for Ki-Hu219M/M. The corrected signal intensities are as follows. Ki-Hu219M/0, 50.7 ± 2.7; Ki-Hu219V/0, 51.8 ± 9.3; and Ki-Hu219V/V, 100.5 ± 13.9/mm² (mean ± S.E.).

gene expression in the homozygous or heterozygous knock-in mice.

Human PrP 219K Molecule Is Conversion-competent in vCJD Infection

At first, we examined the transmission experiment with vCJD prions, since a case of vCJD patient was reported in Japan (29). When considering the possibility of secondary infection from human to human transmission in Japan, it is important to know whether the Japanese populations with the codon 219E/E, E/K or K/K genotype are susceptible to vCJD prions. In secondary vCJD infection, a direct intracerebral route of exposure is only likely to occur during neurosurgical procedures, whereas a peripheral route of infection via blood

transfusion, tissue transplantation or general surgery is far more likely. Thus, we analyzed the susceptibility to vCJD prions using the FDC assay after the peripheral route of infection in a murine model.

It was surprising that positive PrP immunolabeling was observed in the FDC of the spleens from Ki-Hu219K/K intraperitoneally inoculated with vCJD prions (Fig. 2A). To compare the conversion efficiency between PrP 219E and PrP 219K, we prepared knock-in mice with the following genotypes: Ki-Hu219E/K, Ki-Hu219E/0, Ki-Hu219K/0, Ki-Hu219E/E, and Ki-Hu219K/K. These knock-in mice were inoculated with vCJD prions from 2 different patients and were sacrificed at 75 days post-inoculation to analyze PrP^{Sc} in the FDC by immunohistochemistry or Western blotting. The immunohistochemical analysis showed positive FDC staining in almost all knock-in mice inoculated with the vCJD prions (supplemental Fig. S1A). Although the vCJD infection was established in almost all mice irrespective of the codon 219 genotype, the numbers of positively stained FDCs differed in each knock-in mouse (Fig. 2A). Therefore, we counted the total number of lymphoid follicles and the number of positively stained FDCs in all mice. The positive rate in the FDC assay was lowest in Ki-Hu219E/K, followed by Ki-Hu219E/0, Ki-Hu219E/E and Ki-Hu219K/0, and was highest in Ki-Hu219K/K (Fig. 2B). Western blot analysis showed that the quantity of PrP^{Sc} was highest in the spleens of Ki-Hu219K/K, followed by Ki-Hu219K/0, Ki-Hu219E/E and Ki-Hu219E/0, and was lowest in Ki-Hu219E/K (Fig. 2, C and D). Despite the different genotype in the knock-in mice (219K/K) and vCJD prions (219E/E), the most effective conversion was observed in Ki-Hu219K/K mice. Even the hemizygous Ki-Hu219K/0 showed more PrP^{Sc} accumulation than did Ki-Hu219E/E. This observation in Western blot was reproducible in a transmission experiment using another vCJD inoculum (vCJD96/07) (supplemental Fig. S1B). In both transmission experiments, the heterozygous model showed the lowest efficiency of conversion.

Heterozygous Inhibition Is Also Observed in the PRNP Codon 129M/V Genotype—As reported previously (19), Ki-Hu219M/M and Ki-Hu219M/V mice were susceptible to vCJD prions as revealed by FDC assay, but Ki-Hu219V/V mice were not. Because the human PrP 129V molecule is conversion-incompetent in vCJD infection, it was the best model to compare the amount of PrP^{Sc} between Ki-Hu219M/V and Ki-Hu219M/0 to examine the influence of heterozygosity. We prepared knock-in mice with the following genotypes: Ki-Hu219M/V, Ki-Hu219M/0, Ki-Hu219M/M (a synonym for Ki-Hu219E/E), and Ki-Hu219V/V. All of these knock-in mice had Glu at codon 219 of PRNP (Fig. 1A). These mice were inoculated intraperitoneally with vCJD prions (vCJD05/02). In Western blot analysis, Ki-Hu219M/M and Ki-Hu219M/V had PrP^{Sc} in the spleen, but Ki-Hu219V/V did not (Fig. 3, A and B). However, the amount of PrP^{Sc} in the spleens of Ki-Hu219M/V was consistently less than that in Ki-Hu219M/0. This observation in Western blot was reproducible in a transmission experiment using another vCJD inoculum (vCJD96/07) (supplemental Fig. S2). Therefore, the conversion-incompetent human PrP 129V molecule also appears to show an inhibitory effect on the accumulation of human PrP 129M PrP^{Sc}.

Conversion and Inhibitory Effect of PrP 219K

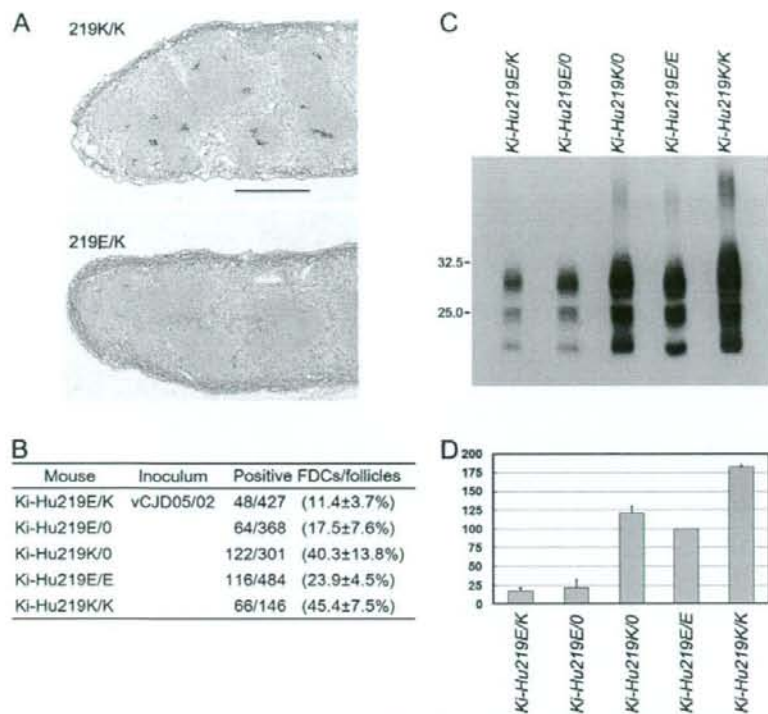


FIGURE 2. Transmission experiment using the knock-in mice with codon 219 polymorphism. *A*, immunohistochemistry analysis of the spleen from Ki-Hu219K/K or from Ki-Hu219E/K. The follicular dendritic cells were positively immunolabeled with PrP antibody. Scale bar, 500 μ m. *B*, summary of the immunohistochemical analysis. We used the hemizygous models (Ki-Hu219E/0 and Ki-Hu219K/0), the homozygous models (Ki-Hu219E/E and Ki-Hu219K/K), and the heterozygous model (Ki-Hu219E/K) intraperitoneally inoculated with vCJD05/02. We counted the total number of positive FDCs and the total number of lymphoid follicles in the spleens from all mice. The positive rate of FDCs for each animal is expressed as mean % value \pm S.D. *C*, Western blot analysis of PrP^{Sc} in the knock-in mice inoculated with vCJD05/02. The position of molecular size standards is shown on the left (kilodaltons). *D*, the comparatively corrected signal intensities (numbers/mm²) are presented. We assigned a signal intensity of 100/mm² for Ki-Hu219E/E. The corrected signal intensities are as follows: Ki-Hu219E/K, 17.6 \pm 3.9; Ki-Hu219E/0, 21.9 \pm 10.1; Ki-Hu219K/0, 121.0 \pm 8.4; and Ki-Hu219K/K, 182.1 \pm 2.1/mm² (mean \pm S.E.).

Transmission Studies via the Intracerebral Administration—It was established that the human PrP 219K molecule is converted in vCJD infection, but it remains uncertain as to whether this molecule could be converted by infection with other prions. To examine the transmissibility of other prions, we performed intracerebral inoculation of 10% brain homogenates from a patient with sCJD. In the transmission experiment using sCJD prions, all Ki-Hu219K/K showed PrP^{Sc} accumulation in the brain. Compared with Ki-Hu219E/E (467 \pm 24 days), Ki-Hu219K/K showed a longer incubation period (573 \pm 103 days) after inoculation with sCJD-MM1 prions (129M/M, 219E/E, and type 1 PrP^{Sc}). It is significant that human PrP 219K could be converted by sCJD-MM1 or MV1 prions (129M/V, 219E/E, and type 1 PrP^{Sc}) (Fig. 4A). Western blot analysis of the brains from Ki-Hu219K/K showed a similar PrP^{Sc} isoform on blot to that seen in Ki-Hu219E/E (Fig. 4B). Thus the human PrP 219K is conversion-competent also in sCJD prion infection.

We also summarize the transmission data of vCJD prions with the intracerebral inoculation (Fig. 4A). In vCJD (vCJD05/02) infection, Ki-Hu219K/K mice showed PrP^{Sc} accumulation in the brain after the incubation period of 412 \pm 6 days.

Ki-Hu219M/M (the same mouse as Ki-Hu219E/E) showed a longer incubation period compared with Ki-Hu219K/K. In addition to these homozygous models, the Ki-Hu219M/V heterozygous mice show no clinical signs and still are alive after >740 days of incubation (Fig. 4A). Therefore, heterozygous inhibition was similarly observed as in intracerebral infections.

DISCUSSION

It was not expected that the Hu219K PrP molecule was converted to the abnormal isoform. Therefore, it should be important to check the protease sensitivity in the normal isoforms and abnormal isoforms of Hu219K and Hu219E. At first, we checked the protease sensitivity of the uninfected or infected brain samples with MM1 prion (supplemental Fig. S3). The pattern in the protease sensitivity of PrP^C and the protease resistance of PrP^{Sc} was almost the same in Ki-Hu219E/E and Ki-Hu219K/K. In addition to this result, the positive rate in the immunohistochemical analysis of the FDC assay infected with vCJD prions correlated to the quantitative data in the Western blot (Fig. 2 and supplemental Fig. S4). In addition, Ki-Hu219K/K mice showed a shorter incubation period compared with Ki-Hu219M/M (Ki-

Hu219E/E) in the central nervous system infection. Therefore, it was concluded that the Hu219K molecule is readily converted in vCJD prions compared with Hu219E. From our data, the Hu219K molecule might be more suitable as a substrate to amplify vCJD prions by the PMCA technique (30) compared with Hu219E (31). Although many transmission studies have shown the importance of homology at the polymorphic codons between PrP^C and PrP^{Sc} for efficient conversion (32), vCJD prions represent an exception as far as *PRNP* codon 219 is concerned. This exception can be explained by the fact that bovine PrP has a amino acid substitution of glutamine corresponding to codon 219. The structure of PrP^{Sc} with Hu219K might have a similar structure of BSE PrP^{Sc} with 219Q compared with that of Hu219E. Based on the codon 219 substitution, we can design a better PrP^C substrate to amplify vCJD prions.

Despite the conversion competence of the Hu219K and Hu219E PrP molecules, heterozygous inhibition was observed in Ki-Hu219E/K as well as Ki-Hu219M/V mice with conversion-competent 129M and conversion-incompetent 129V molecules. In addition to the peripheral route infection in the FDC assay, Ki-Hu219M/V mice showed heterozygous inhibition of

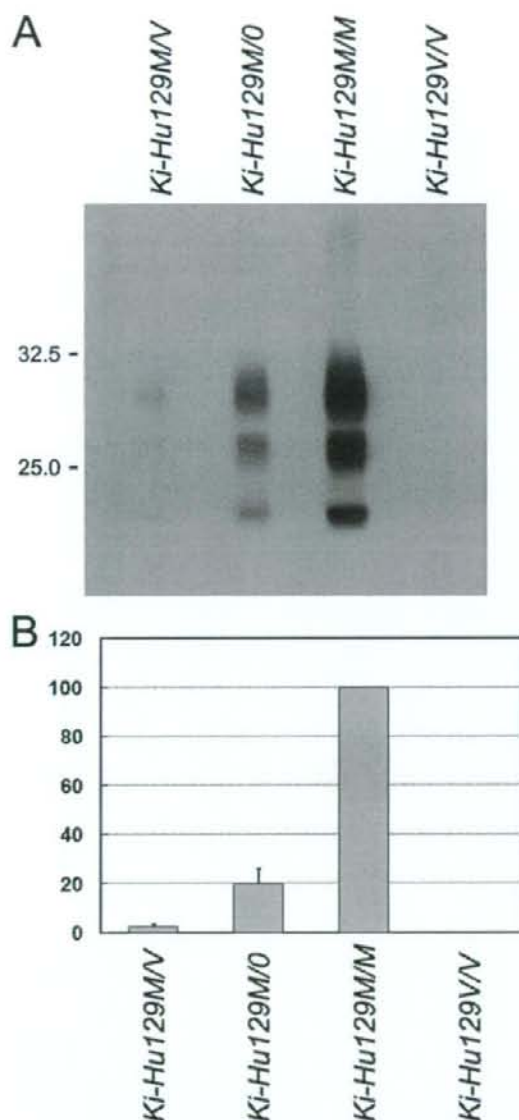


FIGURE 3. Transmission experiment using the knock-in mice with the codon 129 polymorphism. A, Western blot analysis of PrP^{Sc} from the knock-in mice with the 129 polymorphism. The hemizygous model (Ki-Hu129M/O), the homozygous models (Ki-Hu129M/M or Ki-Hu129V/V), or the heterozygous model (Ki-Hu129M/V) were intraperitoneally inoculated with vCJD05/02. The position of molecular size standards is shown on the left (kilodaltons). B, the comparatively corrected signal intensities (numbers/mm²) are presented. We assigned a signal intensity of 100/mm² for Ki-Hu129M/M. The corrected signal intensities are as follows. Ki-Hu129M/V, 2.6 ± 0.7; and Ki-Hu129M/O, 19.7 ± 6.3/mm² (mean ± S.E.).

vCJD prion infection in the central nervous system. Therefore, the heterozygous inhibition is a universal feature of prion infections both in peripheral infection and central nervous system infection.

The effect of *PRNP* polymorphisms have been studied recently in an *in vitro* model (17, 33), in which fibril formation revealed the β -oligomer state (34). It was suggested that the

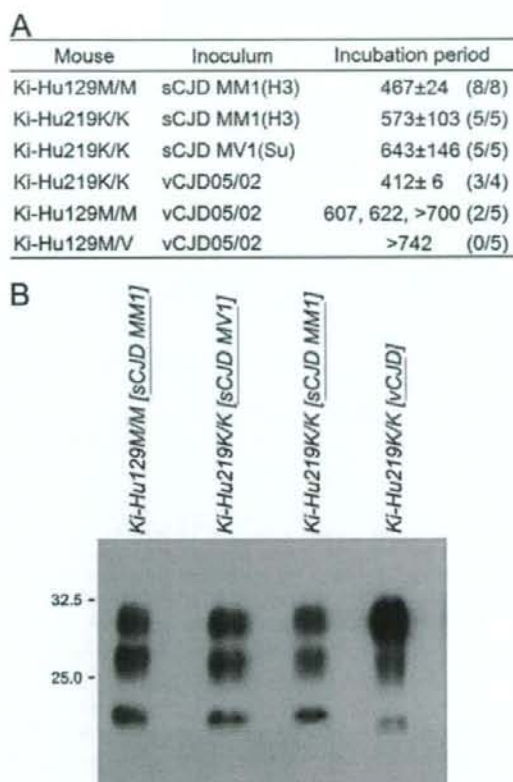


FIGURE 4. Transmission experiment in Ki-Hu219K/K inoculated intracerebrally with sCJD prions. A, summary of the transmission experiments. The MM1 inoculum is the same in both Ki-Hu219K/K and Ki-Hu129M/M. The vCJD inoculum is also the same in Ki-Hu219K/K, Ki-Hu129M/M, and Ki-Hu129M/V. The incubation period was expressed by days (number of positive transmissions/number of total animals). B, Western blot analysis of PrP^{Sc} in the brains. The knock-in mouse [the inoculated sample] is designated above each lane. The position of molecular size standards is shown on the left (kilodaltons).

β -oligomer was not on the pathway to amyloid formation and that the refolding and dissociation of the β -oligomer into the α -monomer most likely preceded the fibril formation. The kinetics of dissociation of the β -oligomer was 100-fold slower in the 129M/V heterogenous β -oligomer than those in either the 129M or 129V homogenous β -oligomer (33). The inhibition of amyloid formation was also reported in a fibrillization model mixed with murine wild-type PrP with 218Q and murine PrP 218K molecule (17). In this system, the murine PrP 218K molecule was converted into a fibril, but the conversion efficiency was lowered. It was interesting that the murine PrP 218K molecules were incorporated into fibrils as often as the wild-type molecules. In another model (35), transgenic mice expressing conversion-incompetent PrP-Fc₂ showed a reduced conversion of wild-type PrP by dimeric PrP-Fc₂. Interestingly, the dimeric PrP-Fc₂ was also incorporated in protease-resistant fibrils.

Based on these previous findings, we propose a possible mechanism to explain the heterozygous inhibition. This mechanism is entirely based on the distinct structure of each PrP^{Sc} molecule (36, 37) (Fig. 5). At first, PrP^C is converted to PrP^{Sc},

Conversion and Inhibitory Effect of PrP 219K

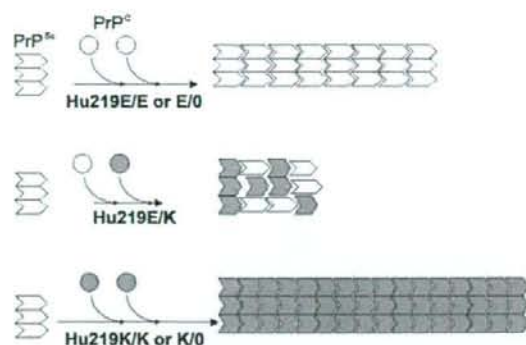


FIGURE 5. A possible mechanism underlying the heterozygous inhibition in vCJD infection. Upper, PrP^{Sc} proliferation model in Ki-Hu219E/E or Ki-Hu219E/O. There is only one PrP^{Sc}. The Hu219E PrP^{Sc} is piled up into the protease-resistant amyloid fibril. Middle, the heterozygous inhibition model. There are two distinct structural PrP^{Sc} in the same mouse. It takes time to pile up amyloid fibrils like a stone fence, because there are two distinct types of PrP^{Sc} blocks. Thus, PrP^{Sc} formation can be inhibited in the heterozygous animals. Lower, PrP^{Sc} proliferation model in Ki-Hu219K/K or Ki-Hu219K/O. The initial seed is Hu219E PrP^{Sc}. However, the resulting Hu219K PrP^{Sc} acts as a new seed, and the increasing Hu219K PrP^{Sc} is piled up rapidly into the protease-resistant amyloid fibrils. There was no or negligible Hu219E PrP^{Sc} as a decelerator. In this figure, each circle or block designates the following: open circles, Hu219E PrP^{Sc}; open hexagonal blocks, Hu219E PrP^{Sc}; filled circles, Hu219K PrP^{Sc}; and filled hexagonal blocks, Hu219K PrP^{Sc}.

then the converted PrP^{Sc} is piled up into amyloid fibrils according to the nucleated polymerization hypothesis (38). In the homozygous and hemizygous animals, there is only one structural PrP^{Sc}. This means that the same blocks (the same structural PrP^{Sc}) are piled up into amyloid fibrils with no other influence on fibril formation and elongation. However, in the heterozygous animals, there are at least two distinct structural PrP^{Sc} composed of the Hu219E or Hu219K molecule. To form and elongate amyloid fibrils in the heterozygous animal, it takes time to pile up amyloid fibrils, because there are two types of blocks (PrP^{Sc}) with a distinct structure (Fig. 5). The two different-shaped PrP^{Sc} may act as decelerators of each other. In the FDC assay of Ki-Hu219M/V, the amyloid fibril formation of Hu219M was inhibited by the Hu219V molecule, which was conversion-incompetent. This phenomenon corresponds to the dominant negative effect as reported previously. We can explain the dominant negative phenomenon by this decelerator hypothesis if the conversion-incompetent Hu219V molecules significantly reduce the rate of Hu219M amyloid formation and elongation.

The decelerator hypothesis may explain some unusual phenomena in prion infections. We propose that PrP^{Sc} molecules with different amino acid sequences act as decelerators in the process of amyloid formation. Because PrP molecules with different amino acid sequences are likely to have different conformations, we can infer that PrP^{Sc} molecules with different conformations act as decelerators in the process of amyloid formation. This decelerator hypothesis can explain the phenomenon described as interference (39), which is observed in an animal inoculated with two different prion strains. A distinct strain should have a distinct conformation of PrP^{Sc}. This PrP^{Sc} with a distinct conformation may inhibit another type of PrP^{Sc} amyloid formation. Recently, it has been reported that the prion interference is due to a reduction of the strain-specific PrP^{Sc}

level (40). Our decelerator hypothesis can account for such prion interference.

In this report, we clearly show heterozygous inhibition of PrP^{Sc} formation using a knock-in mouse model of prion infection. *PRNP* heterozygosity may be important in determining resistance to human prion diseases (12). Although the incubation period after the intracerebral transmission of sCJD prions in Ki-Hu219E/K remains to be determined, the present study suggests that the absence of patients with the 219E/K *PRNP* genotype in sCJD might be due to heterozygous inhibition, because Hu219K is conversion-competent also in sCJD prions infection.

Acknowledgments—We thank H. Kudo and Y. Ishikawa for technical assistance, R.-W. Shin and B. Bell for critical review of the manuscript, and H. Mizusawa for encouraging our activity.

REFERENCES

- Gajdusek, D. C., and Zigas, V. (1957) *N. Engl. J. Med.* **257**, 974–978
- Brown, P., Brandel, J. P., Preece, M., and Sato, T. (2006) *Neurology* **67**, 389–393
- Will, R. G., Ironside, J. W., Zeidler, M., Cousens, S. N., Estibeiro, K., Alperovitch, A., Poser, S., Pocchiari, M., Hofman, A., and Smith, P. G. (1996) *Lancet* **347**, 921–925
- Prusiner, S. B. (1994) *Philos. Trans. R. Soc. Lond. B Biol. Sci.* **343**, 447–463
- Prusiner, S. B. (1998) *Brain Pathol.* **8**, 499–513
- Collinge, J., Palmer, M. S., and Dryden, A. J. (1991) *Lancet* **337**, 1441–1442
- Palmer, M. S., Dryden, A. J., Hughes, J. T., and Collinge, J. (1991) *Nature* **352**, 340–342
- Pocchiari, M., Puopolo, M., Croes, E. A., Budka, H., Gelpi, E., Collins, S., Lewis, V., Sutcliffe, T., Guillivi, A., Delasnerie-Laupretre, N., Brandel, J. P., Alperovitch, A., Zerr, I., Poser, S., Kretschmar, H. A., Ladogana, A., Rietveld, I., Mitrova, E., Martinez-Martin, P., de Pedro-Cuesta, J., Glatzel, M., Aguzzi, A., Cooper, S., Mackenzie, J., van Duijn, C. M., and Will, R. G. (2004) *Brain* **127**, 2348–2359
- Kitamoto, T., and Tateishi, J. (1994) *Phil. Trans. R. Soc. Lond. B* **343**, 319–398
- Jeong, B. H., Lee, K. H., Kim, N. H., Jin, J. K., Kim, J. I., Carp, R. I., and Kim, Y. S. (2005) *Neurogenetics* **6**, 229–232
- Yu, S. L., Jin, L., Sy, M. S., Mei, F. H., Kang, S. L., Sun, G. H., Tien, P., Wang, F. S., and Xiao, G. F. (2004) *Eur. J. Hum. Genet.* **12**, 867–870
- Mead, S., Stumpf, M. P., Whitfield, J., Beck, J. A., Poulter, M., Campbell, T., Uphill, J. B., Goldstein, D., Alpers, M., Fisher, E. M., and Collinge, J. (2003) *Science* **300**, 640–643
- Furukawa, H., Kitamoto, T., Tanaka, Y., and Tateishi, J. (1995) *Mol. Brain Res.* **30**, 385–388
- Shibuya, S., Shin, R.-W., Higuchi, J., Tateishi, J., and Kitamoto, T. (1998) *Ann. Neurol.* **43**, 826–828
- Kaneko, K., Zulianello, L., Scott, M., Cooper, C. M., Wallace, A. C., James, T. L., Cohen, F. E., and Prusiner, S. B. (1997) *Proc. Natl. Acad. Sci. U. S. A.* **94**, 10069–10074
- Perrier, V., Kaneko, K., Safar, J., Vergara, J., Tremblay, P., DeArmond, S. J., Cohen, F. E., Prusiner, S. B., and Wallace, A. C. (2002) *Proc. Natl. Acad. Sci. U. S. A.* **99**, 13079–13084
- Lee, C. I., Yang, Q., Perrier, V., and Baskakov, I. V. (2007) *Protein Sci.* **16**, 2166–2173
- Nishida, Y., Sodeyama, N., Toru, Y., Toru, S., Kitamoto, T., and Mizusawa, H. (2004) *Neurology* **63**, 1978–1979
- Asano, M., Mohri, S., Ironside, J. W., Ito, M., Tamaoki, N., and Kitamoto, T. (2006) *Biochem. Biophys. Res. Commun.* **342**, 293–299
- Kitamoto, T., Mohri, S., Ironside, J. W., Miyoshi, I., Tanaka, T., Kitamoto, N., Itohara, S., Kasai, N., Katsuki, M., Higuchi, J., Muramoto, T., and Shin, R. W. (2002) *Biochem. Biophys. Res. Commun.* **294**, 280–286
- Kobayashi, A., Asano, M., Mohri, S., and Kitamoto, T. (2007) *J. Biol. Chem.*